Journal of Materials Research and Technology 41 (2026) 5188–5204

Contents lists available at ScienceDirect

Journal of Materials Research and Technology

journal homepage: www.elsevier.com/locate/jmrt

# Comparative evaluation of burr formation in low-speed, high-speed and novel laser hybrid high-speed micromilling of Inconel 718

Ahmad Waqar Tehami [a], Muhammad Rizwan ul Haq [a], Muhammad Ali Khan [a,b,*], Syed Husain Imran Jaffery [a,c,**], Muhammad Iftikhar Faraz [d], Jana Petru [e]

[a] School of Mechanical and Manufacturing Engineering (SMME), National University of Sciences and Technology (NUST), Islamabad, 44000, Pakistan

[b] Department of Mechanical Engineering, College of Electrical and Mechanical Engineering (CEME), National University of Sciences and Technology (NUST), Islamabad, 44000, Pakistan

[c] Department of Mechanical Engineering, College of Engineering, Faculty of Computing, Engineering and the Built Environment Birmingham City University, Birmingham, B4 7XG, UK

[d] Department of Mechanical Engineering, College of Engineering, King Faisal University, Al-Ahsa, Saudi Arabia

[e] Department of Machining, Assembly and Engineering Metrology, Mechanical Engineering Faculty, VSB-Technical University of Ostrava, 17, Listopadu 2172/15, Ostrava, 708 00, Czech Republic

A R T I C L E  I N F O

*Keywords:*
Laser machining
Low speed
High speed
Micromachining
Micromilling
Inconel 718
Burr formation

A B S T R A C T

Inconel 718 is a precipitate hardened nickel-based superalloy that has been widely used in the aerospace, power generation and biomedical industries because of its good high temperature strength, corrosion resistance and low cycle fatigue life. However, micro-machining is a difficult process to perform due to its extremely high strength, work-hardening characteristics and abysmally low thermal conductivity that result in unwanted burrs at the micro-level. Systematic comparisons of the behavior of burrs in different domains of machining and especially incorporating hybrid strategies are still limited. To fill this gap, a comparative study of burr formation is pursued in three different micromachining domains: low speed, high speed and a new laser-hybrid high-speed. The experimental study was designed using a Taguchi L16 orthogonal array to investigate the influence of spindle speed, feed, and depth of cut with uncoated and coated tools. Statistical robustness was strengthened using ANOVA to identify the significant effect of each factor on burr growth. It was found that higher spindle speeds are critical for reducing burr formation, and integrating laser assistance demonstrated an even greater suppression. Cutting speed, tool coatings, and feed were reported as the predominant factors in low-speed, high-speed and laser-hybrid high-speed domains, respectively; while depth of cut was identified as a secondary factor in low- and high-speed conditions, with coatings for laser-hybrid machining. The nACo tool had good capability to minimize burrs at low speeds; the uncoated tool performed well for high-speed cutting; and TiAlN was effective in laser-hybrid conditions. The results also confirm the potential of high-speed micromilling, with advances in parameter selection and tool coatings, to achieve superior edge quality and precision.

## 1. Introduction

Miniaturization is a key prerequisite for modern technological development, enabling compact product designs with enhanced functionality. The integration of novel capabilities have driven performance improvements across multiple sectors, including aerospace, automotive, electronics, and biomedical applications [1,2]. Escalating demand for precision-engineered components drives the growth of innovative micromachining technologies to fabricate truly complex and reliable micro-scale features that are vigorous to these industries [3]. Mechanical micromachining has appeared as a highly efficient method for manufacturing complex microstructures with high accuracy and surface integrity in various materials, including Ni-based superalloys [4,5]. This is due to the unique microscale tool–workpiece interactions in

* Corresponding author. Department of Mechanical Engineering, College of Electrical and Mechanical Engineering (CEME), National University of Sciences and Technology (NUST), Islamabad, 44000, Pakistan.

** Corresponding author: School of Mechanical and Manufacturing Engineering (SMME), National University of Sciences and Technology (NUST), Islamabad, 44000, Pakistan.

*E-mail addresses:* mak.ceme@ceme.nust.edu.pk (M.A. Khan), imran@smme.edu.pk (S.H.I. Jaffery).

https://doi.org/10.1016/j.jmrt.2026.02.071
Received 15 January 2026; Received in revised form 8 February 2026; Accepted 8 February 2026
Available online 10 February 2026
2238-7854/© 2026 The Authors. Published by Elsevier B.V. This is an open access article under the CC BY-NC license (http://creativecommons.org/licenses/by-nc/4.0/).

micromilling, a miniaturized form of conventional milling in which the cutting-edge radius and minimum chip thickness are influential process parameters [6]. In demanding environments with a combination of severe heat, mechanical loading and corrosive attack, nickel-based superalloys are irreplaceable [7,8]. Of these, Inconel 718 has wide applications in high performance industries such as aircraft turbines, nuclear reactors, rocket and submarine engines due to its superior strength, thermal stability, and corrosion resistance, which ensure structural integrity at temperatures between 450 °C and 700 °C [9]. The presence of aluminum in Inconel 718 enhances the production of lightweight components with high thermal strength, making this superalloy promising for harsh structural applications [10,11]. On the other hand, due to its high strength and low thermal conductivity, work hardening is more severe during micromachining of Inconel 718, owing to a significant difference in cutting mechanics from conventional manufacturing, which contributes additional heat generation in the cutting zone. In such conditions, it is crucial to optimize machining strategies and tool materials. Among the strategies proposed to improve machinability, tool coating stands out among the most effective solutions. Findings by M. Takács et al. have shown that process-resistant workpiece materials can be processed in great leaps with the use of new coatings. Factors like lower friction coefficients, improved coating hardness and controlled thermal characteristics all combine to provide better cutting results. Such characteristics contribute to tool life and help minimize production costs, while further improving surface quality and shape precision of machined parts [12,13].

Burr generation is still a major obstacle while micromachining, in which burr causes a negative impact on dimensional accuracy and functional reliability of the micro components machined. Although burrs are generated in both macroscale and microscale machining, the control methods are quite different because macroscale and microscale have different size and precision requirements. In traditional macromachining, burrs are typically larger, allowing standard post-processing deburring techniques to be used, which become impractical and complex at the microscale due to tight tolerances and fragile geometries [14,15]. However, in micro-manufacturing, reliance on post-processing is avoided, and alternative burr reduction strategies are focused on in-process control, such as optimal cutting conditions and modified tool geometry, rather than off-line deburring of the machined part [16,17]. The mechanisms responsible for burr evolution in micro end milling are inherently complicated, depending on the localized material deformation and being very sensitive to machining parameters including cutting speed, feed, depth of cut and tool geometry. Given that the burr size is nearby to that of the microfeatures, it is essential to study burr formation, especially in Inconel 718 to advance precision micromachining [18]. In recent years, considerable focus has been directed toward energy-assisted machining techniques such as laser-assisted machining, ultrasonic vibration-assisted machining, electrical discharge machining, and electrochemical machining as a potential approach for processing hard-to-cut superalloys and overcoming precision manufacturing challenges. Among these approaches, laser-assisted hybrid micromachining has emerged as a particularly promising strategy due to its ability to locally modify material behavior while preserving geometric flexibility [19–22]. Nevertheless, Laser Beam Machining (LBM) cannot produce application-ready parts in a single process due to limitations in dimensional control and in the generation of taper profiles [23,24]. Fiber, Nd:YAG, and gas lasers are the choices for selection based on their operational wavelengths and output powers. As reported by J. P. Davim, fine-scale material cleaning and shallow ablation are the most common applications for fiber lasers due to high precision and controllability. The integration of laser systems into contemporary manufacturing processes opens new opportunities in high-value domains, including aerospace and nuclear engineering [25]. This industrial interest stems from the ability of laser systems to provide non-contact, force-free material removal with localized thermal softening and precise delivery, which is particularly beneficial for machining high-strength alloys like Inconel 718. Compared with purely mechanical methods, laser assistance reduces cutting forces, improves process stability, and enhances edge quality, thereby overcoming key limitations of conventional micromachining [22,26,27]. According to Y. Zhang et al., the ablation starts when a substrate absorbs enough thermal energy from the focused laser beam. Localized melting, vaporization, or even thermochemical decomposition occur, once delivered fluence exceeds the material's threshold. This process provides accurate removal of the material and the production of micro-to submicron-sized geometries [28,29].

Hybrid machining techniques have gained prominence owing to their effectiveness in fabricating the miniaturized components from difficult-to-machine materials. By incorporating energy-assisted processes, including ultrasonic vibration, laser heating, and electrical discharge methods, and by adjusting machining parameters to account for material behavior, machinability is improved and mechanical stresses are reduced during processing. Laser Assisted Machining (LAM) is a reflective process in which a focused laser beam irradiates the workpiece material to increase machinability by localized workpiece softening through selective heating. This generates a very thin metamorphic layer that minimizes the adverse effects. Subsequently, mechanical cutting is used to remove the heat-affected zone and maintain the integrity of the materials [30,31]. The experimental study by H. Zhang et al. into laser assisted micromilling of Inconel 718 reported a modest reduction in cutting forces [22]. Hybrid models operate in a sequential or assisted manner to enhance performance and mitigate drawbacks [32,33]. In sequential mode, processing was performed successively on separate platforms which imparts flexibility in operation and ease of customization [34], whereas in assisted mode, two processes operate simultaneously, with one supporting the other, requiring precise coordination between processes and sophisticated equipment needing higher initial capital investment. Recent works by Gupta et al. demonstrate that these hybrid methods can successfully fabricate complex microfeatures, such as holes, channels, and intricate 3D geometries, across diverse materials, including metals, ceramics, and superalloys [35,36].

At the microlevel, fluctuations in material microstructure give rise to non-uniform mechanical responses like tool vibration induced by microhardness variations. These are especially bad at lower feed rates and cutting speeds, resulting in inferior surface texture. The implementation of high-speed machining has become a key factor in shortening production cycles and improving tooling accuracy. Hamdan et al. noted that an optimal combination of feed rate and cutting speed can effectively improve process performance compared to traditional patterns whose cutting mechanics differ [37]. Giasin confirmed the effective applications of higher cutting speed in micromachining [38] and Baig et al. reported that increasing tool speed tends to inhibit built-up edges (BUE), while decreased speed promotes BUE and favors chatter and poor surface finish. He also evaluated burr formation in Inconel 600 at elevated speeds (75–125 m/min) with wet, dry and cryogenic conditions [39]. Siddique et al. carried out a similar parametric investigation for Inconel 718 at moderate speeds (25–75 m/min) to enhance machining responses [40]. In another study, Hasan et al. introduced laser based hybrid micromilling of Ti6Al4V at low cutting speeds (5–10 m/min) to suppress burr formation and identify favorable operating parameters [41]. Additionally, Faraz, Petru, and Sheheryar et al. explored the machinability of Inconel 718 between 9 and 24 m/min using coated and uncoated carbide tools with optimization models [42,43] whereas Giasin extended the investigation to low speeds (8–12 m/min) with similar tooling [38].

Despite extensive research on burr formation in low- and high-speed micromilling of nickel-based superalloys, a significant gap persists because comprehensive investigations systematically compare burr formation mechanisms to facilitate the machinability of Inconel 718 across low-and high-speed and hybrid high-speed micromachining domains remain scarce. Existing studies largely examine mechanical micromilling regimes in isolation, while the role of unconventional processes like laser beam machining (LBM) remains underexplored [44–47]. Particularly, studies that integrate hybrid strategies such as combining laser machining with mechanical micromilling, leaving an incomplete understanding of how these approaches influence burr evolution, suppression and control under varying process conditions. The present study introduces a comparative framework that evaluates burr formation in Inconel 718 across three distinct micromachining domains: low-speed micromilling, high-speed micromilling, and novel laser-hybrid high-speed micromilling, where LBM is employed for pre-conditioning process prior to high-speed micromilling coupled with both uncoated and three different variants of coated micro end mills. The laser stage selectively removes material along the intended cutting path through controlled ablation, reducing the mechanical burden associated with full material engagement and ploughing-domains deformation during subsequent micromilling.

This hybrid strategy synergistically combines the geometric freedom of laser ablation through LBM with the accuracy and flexibility of mechanical micromilling, not only clarifying how machining domain fundamentally governs burr evolution but also demonstrates why hybrid laser-mechanical strategies offer superior edge-quality control compared with purely mechanical approaches. The findings of this study are directly relevant to precision manufacturing sectors where burr suppression is critical to dimensional accuracy, functional performance, and reduction of post-processing costs. Specifically, it is applied in producing high-aspect ratio mold prototypes, micro-textured and micro-patterned surfaces, increasingly demanded in optics, electronics, semiconductors, micro-molding, micro-fluidic systems, microscale fuel cells, micro-chemical reactors, and micronozzles, directly aligning the present comparative and hybrid micromachining study with current industrial trends [48–50]. Moreover, the study establishes a robust experimental and statistical foundation using ANOVA to identify the dominant machining parameters governing burr formation, thereby providing practical guidance for industrial process selection and future development of hybrid micromachining strategies for difficult-to-machine superalloys. The key contributions of this work are summarized as follows:

- Introduction of a novel hybrid micromachining strategy that explicitly integrates laser machining (LBM) as a controlled preconditioning phase prior to mechanical micro-milling, significantly enhancing the machinability of Inconel 718 in the micro-scale domain.
- A systematic and quantitative comparison of burr formation behavior across low-speed, high-speed, and laser-hybrid high-speed micromachining domains, enabling clear identification of domain-dependent dominance of machining parameters governing burr width and burr height.
- Comparative evaluation of uncoated and three advance coated micro-carbide tools (TiAlN, TiSiN, and nACo) elucidated their distinct roles in burr suppression and highlighted the domain-specific tool-process compatibility.
- Implementation of Taguchi L16 orthogonal experimental design to efficiently investigate cutting speed, feed rate, depth of cut and tool coating across four distinct levels, ensuring statistically robust and economically efficient analysis.
- Experimental evidence demonstrates the laser-hybrid high-speed micro-milling provides the most efficient burr suppression, exceeding the improvements achievable through high cutting speeds alone and confirming the synergistic benefit of laser-assisted preconditioning.
- Provision of practical, industry relevant insights that support the adoption of hybrid micro machining strategies to enhance edge quality, reduce burr-related defects, and minimize downstream deburring and finishing operations.

## 2. Materials and methods

The experimental methodology adopted in this work was designed to systematically explore the burr formation behavior of Inconel 718 across three distinct micromachining domains: low-speed micromilling, high-speed micromilling and novel laser-hybrid high-speed micromilling. In the laser hybrid high-speed micromachining domain, the process was implemented in two phases. Laser Beam Machining (LBM) was employed as a preconditioning step prior to mechanical micromilling in the first phase. Laser processing enables non-contact, force-free material removal through controlled thermal ablation, offering clear advantages over purely mechanical cutting when machining high-strength, low thermal conductivity alloys such as Inconel 718. Previous studies by Lauwers et al. have demonstrated that combining laser processing with conventional machining significantly reduces cutting forces and torque due to laser-induced thermal softening of the material [27]. In addition, microhardness evaluations indicate that laser ablation can locally reduce the material strength by up to 30% [26]. By selectively removing the material along the intended cutting path, the laser phase reduces the burden of full material engagement through controlled laser ablation [22] and ploughing-dominated deformation during tool entry and subsequent cutting in second phase. This preconditioning lower edge loading on the micro-tool promotes more stable chip formation and limits excessive plastic flow at the slot edges. Consequently, high-speed micromilling proceeds under more favorable engagement conditions, resulting in improved edge quality, reduced burr generation, and delayed tool wear progression. The integration of laser systems therefore represents a practical and industry-relevant strategy for enhancing micromachining performance where conventional mechanical approaches alone remain insufficient.

The design of experiments was based upon Taguchi L-16 orthogonal array which helps statistically reliable exploration of parameter effects with less experimental runs. Influence of machining parameters namely cutting speed, feed and depth of cut on the burr geometry was evaluated. Uncoated and three kinds of coated tools were operated in micro milling operations. The scheme for experimentation in three domains of machining and framework for response analysis is enlightened in Fig. 1. The use of a comparative framework provided possibilities to directly assess the characteristics of burrs, which were measured and quantified in terms of burr width and burr height across the three machining domains. Subsequent analysis was performed with the use of the analysis of variance (ANOVA) to estimate the statistical significance of input parameters on the burr responses. Verification tests were done against best and worst combination of machining conditions in order to find dependability and repeatability of experimental design. This systematic approach provided not only correlations between input parameters and the burr size, but it also provided a comprehensive comparison of various configurations of micromilling of Inconel 718.

### 2.1. Selection of material

Inconel 718 has become the preferred alloy in highly stressed applications where steel and aluminum fail to maintain structural integrity. It is characterized by very high thermal stability and resistance to corrosion, maintaining mechanical properties across wide temperature spectrum ensuring its suitability as an attractive material in aerospace, power generation, gas turbine and nuclear application systems [51,52]. These features also render Inconel 718 well known for its poor machinability, such that it represents a suitable material to study and test advanced and hybrid micromachining processes targeting at improved machinability while retaining intact the inherent performances of the alloy. Table 1 exhibits a comparative overview of the mechanical properties of the Inconel 718 with some aerospace alloys.

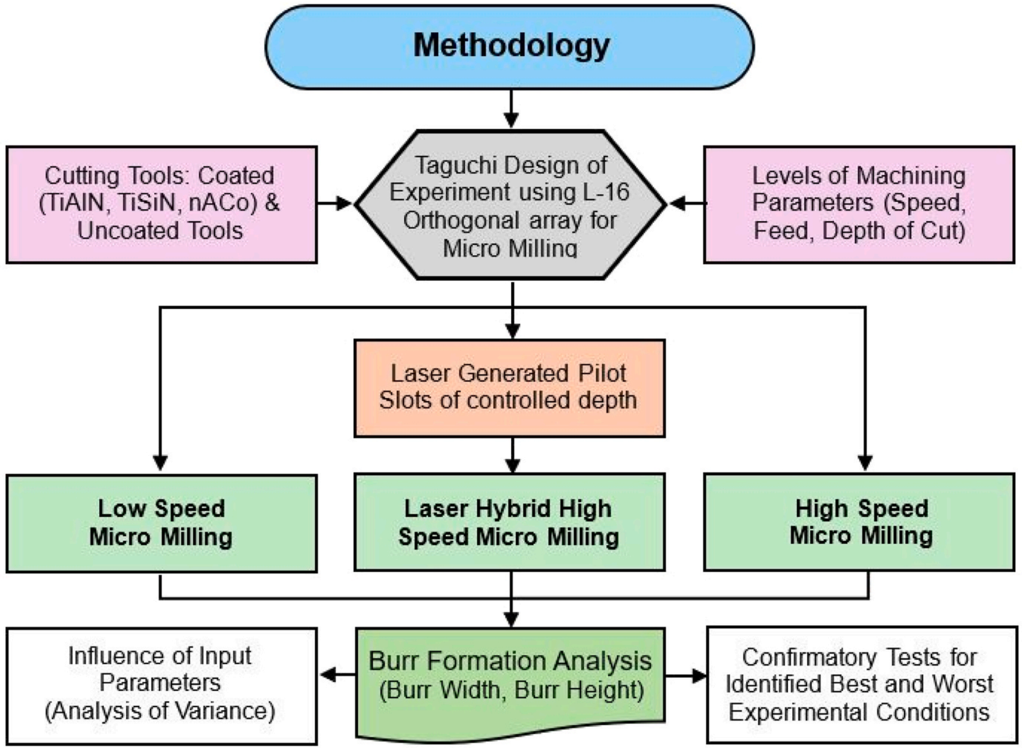


**Fig. 1.** Scheme of experimental procedure and subsequent analysis.

**Table 1**
Mechanical properties of Aerospace alloys.

| | Ti–6Al–4V | Monel 400 | Inconel 600 | Inconel 718 |
|---|---|---|---|---|
| **Density (g/cm$^3$)** | 4.5 | 8.8 | 8.4 | 8.2 |
| **Hardness (HB)** | 320 | 110–150 | 360 | 390 |
| **Tensile strength (MPa)** | 950 | 512–620 | 1050 | 1600 |
| **Elastic modulus (GPa)** | 113.8 | 179 | 205 | 205 |
| **% Elongation** | 14 | 48 | 25–30 | 15 |
| **Thermal conductivity (W/m.K)** | 6.7 | 21.8 | 10 | 11.4 |

### 2.2. Specifications of cutting tools

Ezugwu et al. emphasized that tools used for nickel-based superalloys must possess very high hot hardness, resistance to wear, mechanical strength and toughness as well as chemical inertness at high temperatures [53]. When micro-milling Inconel 718 is considered, an overall tool material evaluation becomes mandatory since its performance is highly dependent on both the intrinsic physical features of materials, operation conditions and tool geometry. The fact that Inconel 718 is an abrasive workpiece material, in conjunction with its extreme high temperature tolerance, imposes large thermo-mechanical loads on cutting tools leading to impulsive wear and operational lifespan reduction [13,54]. To have a systematic comparison of the performance, both uncoated tools and coated counterparts were tested. The latter contains sophisticated protective coatings of Titanium Silicon Nitride (TiSiN), Titanium Aluminum Nitride (TiAlN), and an AlTiSi based nanocomposite (nACo). Fig. 2 shows the geometrical characteristics and coating conditions of the used tools.

Two-flute square end carbide mill of 500 μm diameter from North Carbide Tools was used for micro-milling operations in all the three domains of machining in this study. The tool material chosen was tungsten carbide because of its high mechanical strength and wear resisting property. It had an overall length of 50 mm and a Rockwell hardness of 60 HRC which significantly increases durability toward cutting wear. Additionally, the tool was designed with a helix angle of 30° which facilitates effective chip evacuation and improves machining efficiency.

Table 2 outlines the technical specifications of the coatings procured from North Carbide Tools [38]. The average cutting-edge radius measurements were recorded as 2.73 μm for TiAlN, 2.87 μm for TiSiN, 2.66 μm for the nanocomposite nACo, and 2.57 μm for the uncoated tool. To ensure reliability of outcomes and eliminate the influence of prior wear, an unused tool was employed for each experimental machining trial.

### 2.3. Preparation of workpiece

A rectangular specimen of Inconel 718 measuring 10 mm × 10 mm × 50 mm was rigidly fixed in a precision vice to ensure stability during processing. The top face was initially leveled using a carbide end mill of 12 mm diameter to generate a precise datum surface to guide subsequent laser slotting in laser hybrid approach and further mechanical micro-milling in all three domains. Without altering the clamping setup, the same specimen was then transferred to the micro-milling platform, where mechanical machining was performed. The experimental protocol consisted of producing slots of 10 mm length, arranged at an inter-slot distance of 3 mm, as illustrated in Fig. 3.

### 2.4. Laser machining equipment

The hybrid process of laser assisted mechanical micro-milling integrates laser technology to enhance machining precision. The process was initiated through the generation of pilot slots on the pre-machined Inconel 718 specimen using a fiber laser system with a rated output of 20 W. The fiber laser configuration Raycus/IPG optional produced by Maxphotonics as depicted in Fig. 4, is capable of achieving a depth up to 0.5 mm. Control over slot geometry was achieved by varying operating parameters of laser such as laser power, frequency and scanning speed with the help of an inbuilt Graphical User Interface (GUI) provided by the Ezcad2 software.

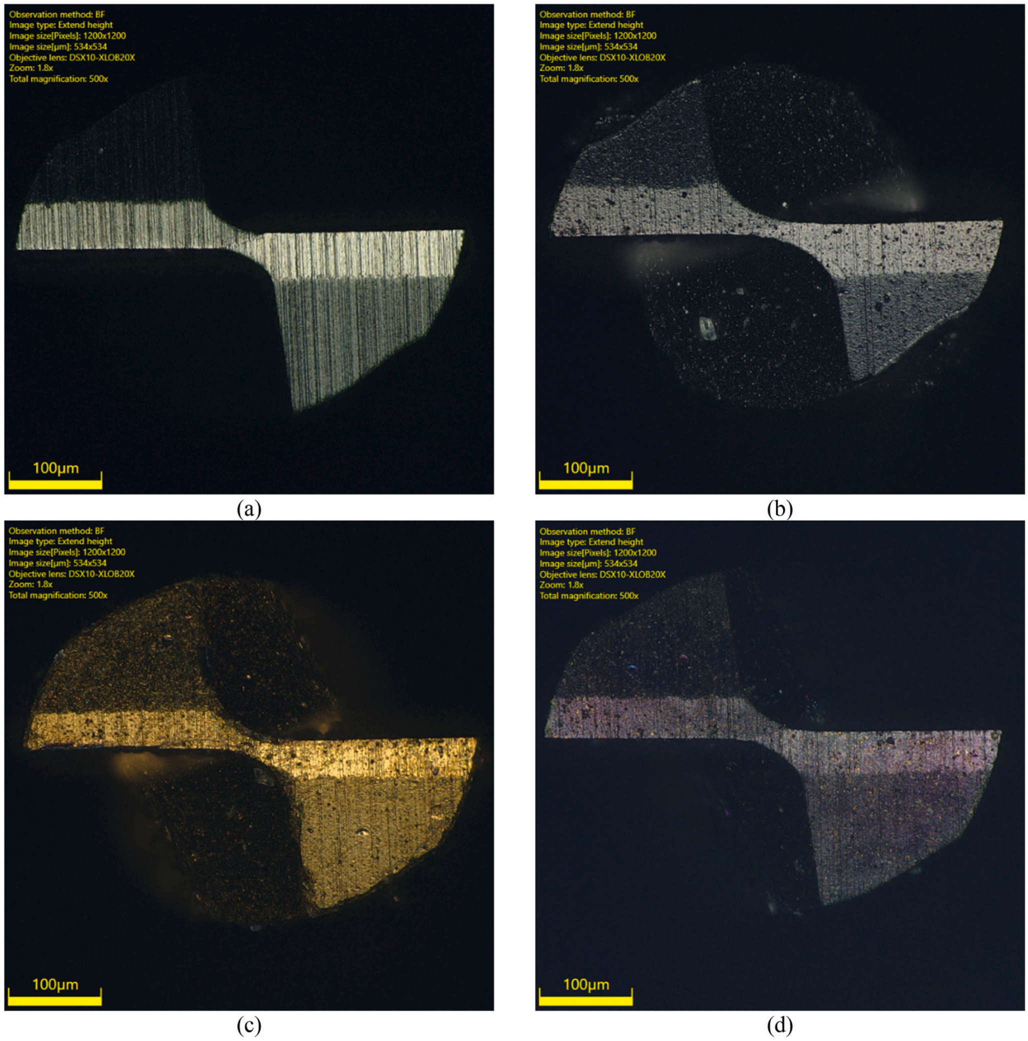


**Fig. 2.** Uncoated and Coated Tools: (a) Uncoated; (b) TiAlN-coated; (c) TiSiN-coated; (d) nACo-coated.

**Table 2**
Details of the coating specifications.

| Specification | AlTiN | TiSiN | nACo |
|---|---|---|---|
| **Hardness (HV)** | 3200 | 3600 | 4500 |
| **Thickness (microns)** | 2.5–3 | 3 | 3 |
| **Oxidation temp (∘C)** | 900 | 1000 | 1200 |
| **Coefficient of Friction** | 0.3 | 0.45 | 0.4 |
| **Color** | Black | Golden | Blue |

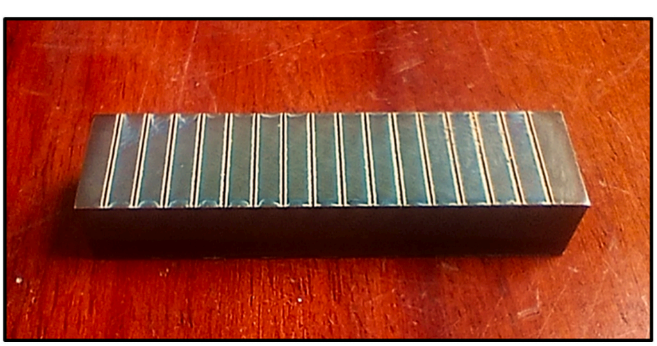

**Fig. 3.** Inconel 718 specimen used in the study.

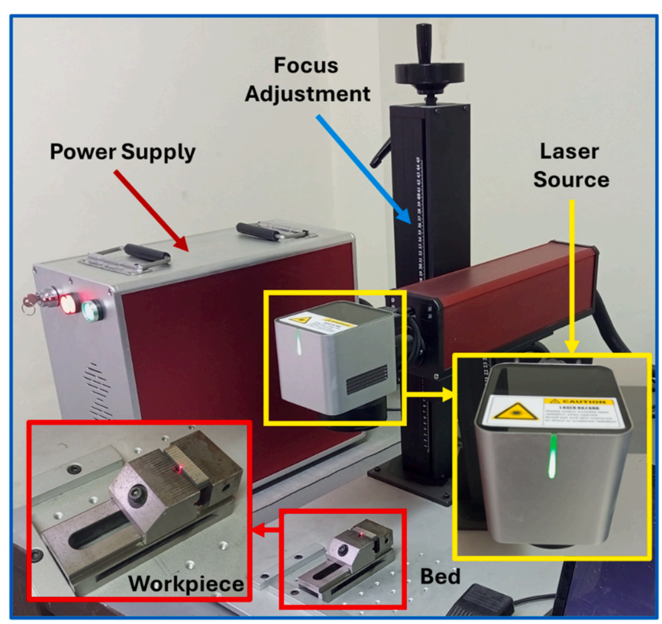


**Fig. 4.** Laser machining equipment.

The laser system allowed a minimum spot diameter of 0.01 mm, scanning speed up to 7000 mm/s and positioning repeatability of ±0.003 mm. The optical system was designed with a focal length of 87 mm to be accurate for the beam when processing. Prior to finalization of the machining conditions, a preliminary parameter screening was conducted to investigate the influence of process parameters such as power level, frequency value, scan speed and number of loop passes on pilot slot geometry. In the analysis, slot depth was reserved to be a key factor and slot width has been regarded as another. Based on these preliminary results, an adequate combination of parameters to obtain target slot depths was translated so as to be capable of achieving target slot depths with a high level of accuracy. To facilitate successful hybrid machining, the depth of laser-induced pilot slots were intentionally set to be 10 μm shallower than the target depths for micro-milling operation. For example, a 50 μm laser slot was created before milling a 60 μm machining slot. Fig. 5 shows representative pilot slots with corresponding parameter conditions. Higher pulse frequencies enabled the laser to generate more uniform and consistent pilot slots with lower variation, whereas low frequencies resulted in recast layers forming because of poor localized energy, resulting in irregular melting.

### 2.5. Setup for milling operation

Once the pilot slots were milled, the workpiece was then machined to its final depth on a high precision 3-axis vertical mill center (YDPM Model MV-1060), as presented in Fig. 6(a). The milling operation presented in Fig. 6(b), was performed with care to ensure the dimensional accuracy and stable processing. Further, all the machining experiments were performed by the Taguchi experimental design presented in Section 2.6. To maintain the position accuracy when the laser machining is followed by milling, the sample was clamped first in 2 inch precision vice before removing material by laser. Not only positional accuracy was achieved in transferring specimen on the milling center but also, this strategy successfully minimized the vibration that results in a negative impact on micro-milling slot geometry. Calibrations of the Z-axis were conducted by BMD Messwell 410V tool pre-setter that are required for hybrid micromachining processes with micron level of measurement accuracy and can be seen in Fig. 6(c).

### 2.6. Taguchi design of experiments

Unreasonable choice of machining parameters results in tool degradation, compromises tool longevity and destabilizes the process which is even more significant in micromilling. For stable processing and dependable machining results, the critical milling parameters require to be efficiently optimal adjusted [11]. Optimization of parameters stabilizes the process and guarantees reliable outcomes across multiple machining environments. In this context, the Taguchi experimental design has attracted significant attention due to its employment of orthogonal arrays for a systematic parameter examination without exhaustive full factorial experimentation. The advantage of this approach is the reduction in the number of actual experiments while retaining statistical accuracy and increasing process robustness as well as avoiding environmental or material variations [55]. In the current work, a Taguchi L16 orthogonal array has been planned to study four significant factors: cutting speed, feed rate, depth of cut and tool coating type. Each process parameter was investigated at four distinct levels, shown in Table 3, to ensure sufficient coverage of the operating domain and to capture potential nonlinear and transition behaviours characteristic of micro-milling of Inconel 718. The input ranges of the process parameters: low spindle speed (6-10.5 m/min), high spindle speed (50-125 m/min), feed per tooth (0.5-3.5 μm/tooth), and depth of cut (60-150 μm), were selected to span both speed domains and the micro-milling scale where minimum uncut chip thickness, ploughing–-shearing transition, tool–workpiece contact mechanics, burr formation sensitivity, and surface integrity evolve significantly. Similar parameter windows have been reported in prior micro-milling studies on Inconel 718 and comparable high-strength alloys with comparable cutting tools and scale [38–40,56]. Specifically, feed per tooth range are chosen to distinguish the three micro-milling regimes: ploughing, transition, and shearing. This design allows investigation of the coating and tool performance under both size-effect dominated and conventional cutting conditions, following the methodology adopted in prior micro-milling studies done by Aramcharoen & Mativenga [57], de Oliveira et al. [58], Anand-Krishnan & Mathew [59] and Syed Jaffery [60]. This four-level scheme offers adequate resolution to meaningful identification of trends while maintaining feasible experimental cost. It integrates all the machining domains into single comparative context along with fixed values of feed rate, cutting depth and tool coating conditions to ensure uniformity for meaningful cross-domain comparison.

Contrasting to full factorial design which would require 256 experiments for four parameters at four levels, utilizing the Taguchi fractional factorial scheme required only 16 trials per domain which is highly efficient. Three machining domains were tested for a total of 96 experiments. Confirmatory testing was conducted to verify the robustness of these observations in all instances, with an additional 18 runs. Burr size was selected as the response variable and subsequent effects of different cutting condition factors such as a range of speed levels, feed levels (below, equal to, and above the cutting-edge radius), several cutting-depths, and tool types (uncoated and coated) were

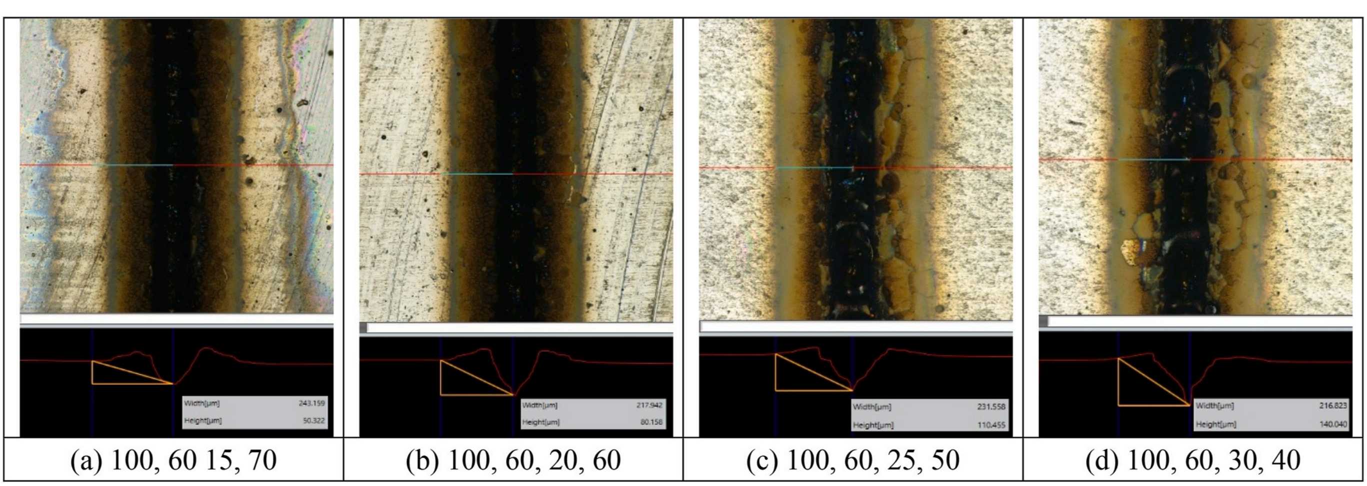


**Fig. 5.** Laser generated pilot slots for depth levels: (a) 50 μm; (b) 80 μm; (c) 110 μm; (d) 140 μm, using defined parameters (Power, Frequency, Loop Count, Scan Speed).

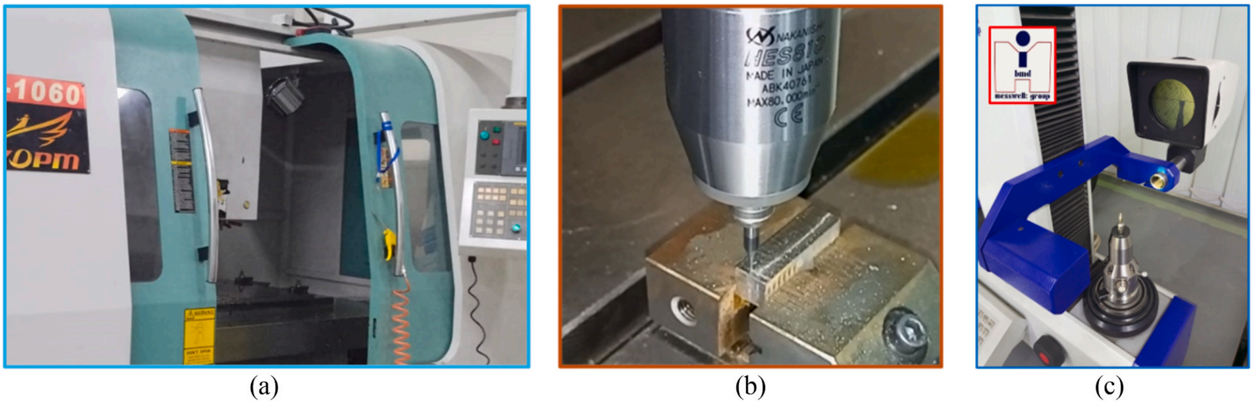


**Fig. 6.** Experimental setup components: (a) Vertical milling machine; (b) Machining operation; (c) Tool Pre-setter.

**Table 3**
Levels of process parameters in micromilling across domains.

| Input parameters | Level 1 | Level 2 | Level 3 | Level 4 |
|---|---|---|---|---|
| **High Speed Domain ($V_c$, m/min)** | **50** | **75** | **100** | **125** |
| **Low Speed Domain ($V_c$, m/min)** | **6** | **7.5** | **9** | **10.5** |
| **Feed ($f_z$, µm/tooth)** | 0.5 | 1.5 | 2.5 | 3.5 |
| **Depth of Cut ($ap$, $\mu$m)** | 60 | 90 | 120 | 150 |
| **Tool Coatings** | Uncoated | TiAlN | TiSiN | nACo |

analyzed. To further assess the significance and relative impact of each factor, ANOVA was utilized as a useful tool to gain an understanding of the most influencing parameters affecting process performance.

Meta-heuristic optimization techniques such as Genetic Algorithms, Particle Swarm Optimization, Non-Dominated Sorting Genetic Algorithm II, and Grey Wolf Optimizer are powerful tools applied for solving complex, nonlinear, and multi-objective optimization problems in machining and manufacturing [61–63], and have been shown to effectively explore global optima in large search spaces. However, these approaches typically require a large number of function evaluations or iterations to converge and extensive computational or surrogate modeling, which are particularly effective in simulation-based studies but impose substantial experimental burden associated with physical machining trials and cost constraints when applied on high-cost alloys such as Inconel 718 [64,65].

### 2.7. Measurement of responses

Burr generation in micro-milling manifests in several distinct forms namely top, entrance, exit and bottom burrs depending on tool

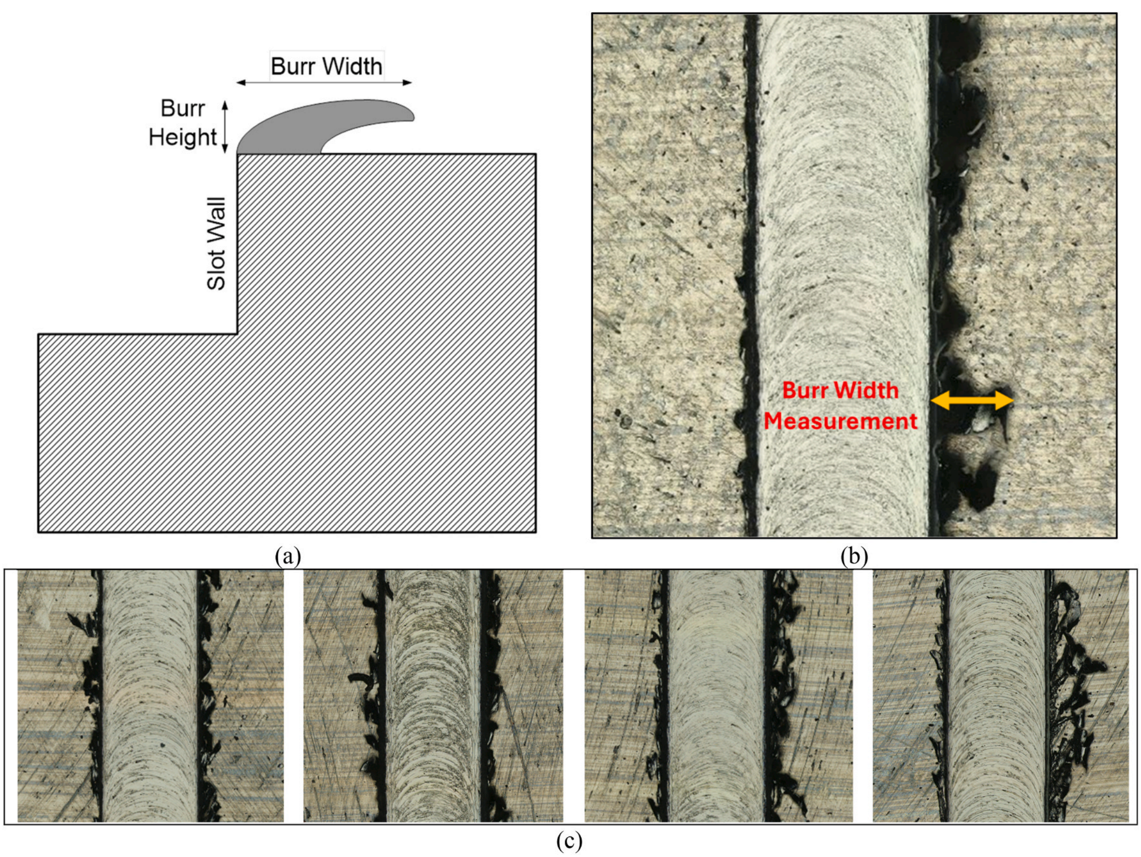


**Fig. 7.** Burr Width: (a) Measurement approach; (b) Measurement of burr width; (c) Representative micrographs.

engagement mechanics and cutting path orientation. Chips produced in the course of micromilling move upwards along the rake face of the tool, inducing the material that is influenced by chips and workpiece to be detached at high tensile stresses. A portion of this deformed material remains adhered to the top surface instead of being removed with the chips, leading to the formation of top burrs [66]. The top burr has been considered in this study. In Fig. 7(a), the approach for the measurement of both the top burr metrices is illustrated while Fig. 7(b) and (c) presents the measurement of burr width by enumerating horizontal length of the burr relative to the slot wall and representative micrographs, respectively [16].

Experimental evidence has demonstrated that the burr formation is much more severe on the down-milling side, a trend largely attributed to low instantaneous cutting-edge velocity with respect to the up-milling arrangement and it is consistent with observation made by Syed H. Imran Jaffery [60]. For the present work, maximum value of top burr width and height on the down-milling edge of each slot were measured with a digital microscope (DXS-1000, OLYMPUS, Tokyo, Japan) as shown in Fig. 8(a), under different magnifications by using microscope's integrated OLYMPUS stream software DSX-BSW version 1.1.5 shown in Fig. 8(b).

The corresponding burr sizes, indicating the burr formation status in three machining domains: low-speed, high-speed and laser hybrid-high speed are presented in Table 4 against the burr width and Table 5 as for the burr height, which fairly compare the performance of burr response under various processing conditions.

## 3. Results and discussions

To reduce the effect of tool wear, every experimental condition was replicated twice under identical settings using a new tool for each trial. The experimental results are summarized in Tables 4 and 5 against burr width and height, respectively. Concerning micromachining, being a highly sensitive technology, even minor deviations and inaccuracies have a considerable impact on the result. The minor deviations observed between successive runs were primarily linked to operator error, tool variability and inherent machine noise.

### 3.1. Application of ANOVA

To examine the statistical significance of factors, ANOVA was applied [55], using the lower-the-better principle [20] to compute contribution ratios and rank parameter influence. This was executed by calculating the sequential sum of squares ($SS_A$) for every parameter using Equation (1).

$$SS_A = \sum_{i=1}^{3} \frac{A_i^2}{n} - \frac{\left(\sum_{j=1}^{N} T_j\right)^2}{N} \quad (1)$$

Where, $i$ is level, $A$ is processing parameter, $j$ is number of runs, $n$ is the total number of runs at a specific level, $T$ is value of response at each run, and $N$ is the total number of runs. Total sum of squares ($SS_T$) and Sequential sum of squares of error ($SS_e$) can be established using Equation (2) and Equation (3).

$$SS_A = \sum_{i=1}^{3} \frac{A_i^2}{n} - \frac{\left(\sum_{j=1}^{N} T_j\right)^2}{N} \quad (2)$$

$$SS_e = SS_T - \sum_{i=A}^{Z} SS_i \quad (3)$$

The parameter with the high F-value signifies its high impact on output responses. The percentage contribution or contribution ratio (*% CR*) of individual parameters can be determined by Equation (4).

$$\%CR = \frac{SS - (df \text{ x } MSS_{Res})}{SS_T} \text{ x } 100 \quad (4)$$

The parameters with *p-values* below 0.05 were regarded as statistically meaningful at the 95% confidence interval [67]. Validation experiments were performed with the most and least favorable parameters settings to validate the predictions made by ANOVA. These results clearly demonstrate that successful optimization of micromilling process for Inconel 718 requires understanding of material response, tool wear and parameter interactions [54,68–70].

### 3.2. Contribution of process variables

#### 3.2.1. Burr width analysis

The contribution of the input factors to burr width for low-speed, high-speed and laser hybrid high-speed micromilling domains are summarized in Table 6. At low speed, cutting speed played a major role with an effect percentage of 32.41%, followed by depth of cut (26.00%), while feed rate (13.88%) and coatings (12.22%) showed relatively less effects. This suggests that at lower cutting speeds, burr formation is highly influenced by material removal rate and thermal-mechanical interaction related to the speed and depth of cut. In the domain of high-speed machining, the relative influence of process variables shifted towards tool coatings (26.42%) and depth of cut (25.69%), surpassing cutting speed (22.84%) in significance, while feed reported 20.28% influence. The enhanced influence of the coatings under these conditions emphasizes the importance of thermal stability, hardness and

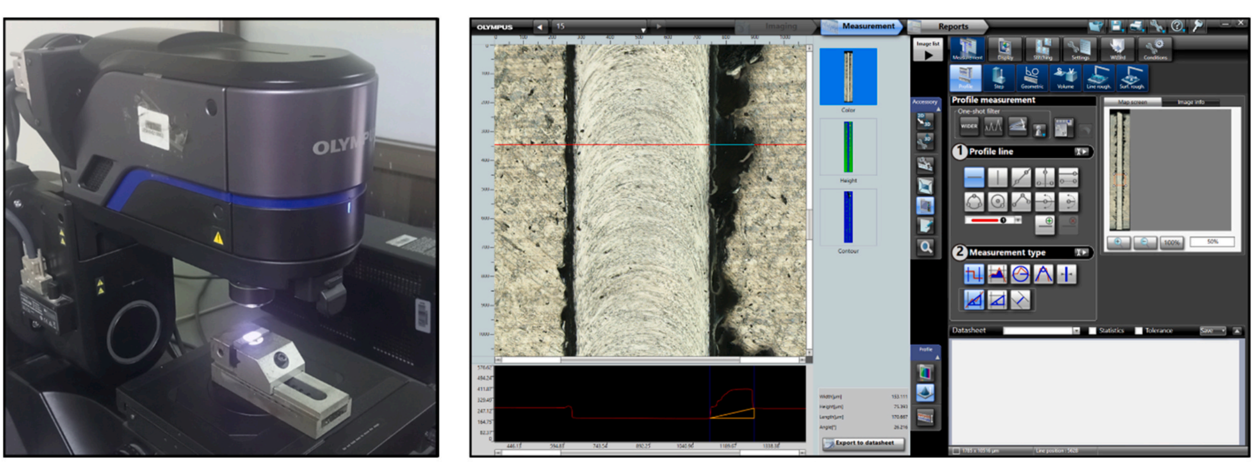


(a) (b)

**Fig. 8.** Measurement configuration: (a) Digital Microscope DSX-1000; (b) Measurement of burr width.

**Table 4**
Taguchi L-16 orthogonal array of process parameters along with corresponding burr widths.

| Test | Input Parameters Common to Both Speed Domains | | | Response Parameter for High and Low Speed Domains | | | | | |
|---|---|---|---|---|---|---|---|---|---|
| | Feed fz | DoC ap | Tool Coating | Domain (LSM) | | Domain (HSM) | | Domain (L-HSM) | |
| | | | | Low Speed (Input) | Burr Width | High Speed (Input) | Burr Width | Laser- High Speed | Burr Width |
| | (μm/th) | (μm) | (t_c) | (m/min) | (μm) | (m/min) | (μm) | (m/min) | (μm) |
| 1 | 0.5 | 60 | UCoat | 6 | 192.03 | 50 | 126.13 | 50 | 130.21 |
| 2 | 1.5 | 90 | TiAlN | 6 | 179.23 | 50 | 153.97 | 50 | 109.42 |
| 3 | 2.5 | 120 | TiSiN | 6 | 273.38 | 50 | 202.03 | 50 | 180.22 |
| 4 | 3.5 | 150 | nACo | 6 | 256.19 | 50 | 128.67 | 50 | 82.51 |
| 5 | 0.5 | 90 | TiSiN | 7.5 | 243.72 | 75 | 148.29 | 75 | 143.2 |
| 6 | 1.5 | 60 | nACo | 7.5 | 221.73 | 75 | 145.11 | 75 | 151.17 |
| 7 | 2.5 | 150 | UCoat | 7.5 | 409.63 | 75 | 192.13 | 75 | 159.84 |
| 8 | 3.5 | 120 | TiAlN | 7.5 | 295.81 | 75 | 166.16 | 75 | 76.37 |
| 9 | 0.5 | 120 | nACo | 9 | 288.06 | 100 | 199.17 | 100 | 176.29 |
| 10 | 1.5 | 150 | TiSiN | 9 | 256.17 | 100 | 224.71 | 100 | 184.08 |
| 11 | 2.5 | 60 | TiAlN | 9 | 251.43 | 100 | 249.04 | 100 | 123.29 |
| 12 | 3.5 | 90 | UCoat | 9 | 341.09 | 100 | 102.08 | 100 | 105.41 |
| 13 | 0.5 | 150 | TiAlN | 10.5 | 279.14 | 125 | 166.23 | 125 | 137.18 |
| 14 | 1.5 | 120 | UCoat | 10.5 | 204.07 | 125 | 139.21 | 125 | 124.86 |
| 15 | 2.5 | 90 | nACo | 10.5 | 130.71 | 125 | 111.26 | 125 | 88.54 |
| 16 | 3.5 | 60 | TiSiN | 10.5 | 221.39 | 125 | 157.14 | 125 | 113.68 |

**Table 5**
Taguchi L-16 orthogonal array of process parameters along with corresponding burr heights.

| Test | Input Parameters Common to Both Speed Domains | | | Response Parameter for High and Low Speed Domains | | | | | |
|---|---|---|---|---|---|---|---|---|---|
| | Feed fz | DoC ap | Tool Coating | Domain (LSM) | | Domain (HSM) | | Domain (L-HSM) | |
| | | | | Low Speed (Input) | Burr Height | High Speed (Input) | Burr Height | Laser- High Speed | Burr Height |
| | (μm/th) | (μm) | (t_c) | (m/min) | (μm) | (m/min) | (μm) | (m/min) | (μm) |
| 1 | 0.5 | 60 | UCoat | 6 | 133.98 | 50 | 107.19 | 50 | 94.23 |
| 2 | 1.5 | 90 | TiAlN | 6 | 202.92 | 50 | 101.03 | 50 | 42.18 |
| 3 | 2.5 | 120 | TiSiN | 6 | 243.09 | 50 | 206.61 | 50 | 107.11 |
| 4 | 3.5 | 150 | nACo | 6 | 228.23 | 50 | 116.62 | 50 | 46.83 |
| 5 | 0.5 | 90 | TiSiN | 7.5 | 192.03 | 75 | 127.58 | 75 | 88.95 |
| 6 | 1.5 | 60 | nACo | 7.5 | 157.32 | 75 | 142.07 | 75 | 125.27 |
| 7 | 2.5 | 150 | UCoat | 7.5 | 288.37 | 75 | 145.03 | 75 | 62.32 |
| 8 | 3.5 | 120 | TiAlN | 7.5 | 127.29 | 75 | 94.01 | 75 | 39.88 |
| 9 | 0.5 | 120 | nACo | 9 | 174.58 | 100 | 118.01 | 100 | 111.37 |
| 10 | 1.5 | 150 | TiSiN | 9 | 218.31 | 100 | 157.63 | 100 | 150.77 |
| 11 | 2.5 | 60 | TiAlN | 9 | 217.09 | 100 | 109.37 | 100 | 86.13 |
| 12 | 3.5 | 90 | UCoat | 9 | 247.67 | 100 | 54.17 | 100 | 71.98 |
| 13 | 0.5 | 150 | TiAlN | 10.5 | 183.77 | 125 | 113.57 | 125 | 122.06 |
| 14 | 1.5 | 120 | UCoat | 10.5 | 133.23 | 125 | 98.49 | 125 | 89.41 |
| 15 | 2.5 | 90 | nACo | 10.5 | 114.37 | 125 | 74.43 | 125 | 70.37 |
| 16 | 3.5 | 60 | TiSiN | 10.5 | 151.13 | 125 | 111.37 | 125 | 99.25 |

tribological behavior of tool surfaces for suppress burr evolution at high speeds. The proximity effects of coatings and depths of cut also indicate a coupled mechanism, where the coatings mitigate the increased mechanical and thermal stresses from deeper engagements.

For the laser hybrid high-speed domain, it can be seen that the sequence turned clearly around, with feed (37.05%) having primary effects and coatings (26.24%) of secondary effect, whereas the effects of the speed (14.87%) and depth of cut (10.16%) are being followed. The role of feed in this field can be explained with the help of localized softening with laser assistance, and the decrease of the cutting resistance that causes the shift of the burr formation sensitivity towards chip load per tooth. Coating was found to be important in order to point out the synergy of the action to preserve the edge integrity from both thermal and vibrational fields. The relatively lower influence of depth of cut and speed is explained in reference to the stabilizing effect of the hybrid energy input on the reduction of direct contribution to burr generation.

In summary, the trends reveal a domain-specific evolution of parameter influence across both burr metrics as illustrated in Fig. 9(a) and (b). Cutting speed dominates at low speed, tool coatings gain prominence at high speed, and feed becomes critical under laser hybrid conditions. These deviations are consistent with physics of underlying mechanisms for each domain: thermal-mechanical equilibrium at low speed, material-tool interaction and tribology at high speed and energy-assisted softening for the hybrid case. These findings highlighted the requirement for domain-specific parameter optimization techniques for efficient burr suppression of Inconel 718 micromachining.

### *3.2.2. Burr height analysis*

Statistical significance of each process parameter for burr height is presented in Table 7 for low-speed, high speed and laser hybrid high-speed micromilling. Under low-speed conditions, cutting speed is the major affecting parameter (28.54%) followed closely by depth of cut (27.61%). Feed (12.21%) and coatings (7.81%) showed relatively less importance. This ranking is consistent with the results for burr width at low speed, where cutting speed was also found to be the predominant factor controlling burr formation at lower machining speeds.

In the high-speed domain, rank levels of parameters display a shearing manner with respect to burr width. The coatings have been observed once more with the largest interference (37.96%), followed by the depth of cut (25.92%), while feed (16.62%) and speed (13.76%) do not play a significant role. The ranking is very close to that in burr width, only with small numerical differences of contribution numbers, which

**Table 6**
Significance and contribution of process parameters for burr width.

| Source | DF | Seq SS | Contribution | Adj SS | Adj MS | F-Value | P-Value |
|---|---|---|---|---|---|---|---|
| ANOVA at Low Speed | | | | | | | |
| Speed | 3 | 42191 | 32.41% | 42191.1 | 14063.7 | 13.26 | 0.000 |
| Feed | 3 | 18073 | 13.88% | 18072.6 | 6024.2 | 5.68 | 0.006 |
| DoC | 3 | 33838 | 26.00% | 33838.0 | 11279.3 | 10.63 | 0.000 |
| Coatings | 3 | 15905 | 12.22% | 15904.9 | 5301.6 | 5.00 | 0.010 |
| Error | 19 | 20159 | 15.49% | 20158.5 | 1061.0 | | |
| Total | 31 | 130165 | 100.00% | | | | |
| ANOVA at High Speed | | | | | | | |
| Speed | 3 | 11466.4 | 22.84% | 11466.4 | 3822.12 | 30.31 | 0.000 |
| Feed | 3 | 10179.4 | 20.28% | 10179.4 | 3393.14 | 26.90 | 0.000 |
| DoC | 3 | 12897.6 | 25.69% | 12897.6 | 4299.19 | 34.09 | 0.000 |
| Coatings | 3 | 13261.3 | 26.42% | 13261.3 | 4420.42 | 35.05 | 0.000 |
| Error | 19 | 2396.3 | 4.77% | 2396.3 | 126.12 | | |
| Total | 31 | 50200.9 | 100.00% | | | | |
| ANOVA at Laser Hybrid High Speed | | | | | | | |
| Speed | 3 | 5088.5 | 14.87% | 5088.5 | 1696.15 | 8.07 | 0.001 |
| Feed | 3 | 12678.0 | 37.05% | 12678.0 | 4225.99 | 20.10 | 0.000 |
| DoC | 3 | 3476.9 | 10.16% | 3476.9 | 1158.95 | 5.51 | 0.007 |
| Coatings | 3 | 8978.7 | 26.24% | 8978.7 | 2992.92 | 14.24 | 0.000 |
| Error | 19 | 3994.7 | 11.67% | 3994.7 | 210.25 | | |
| Total | 31 | 34216.8 | 100.00% | | | | |

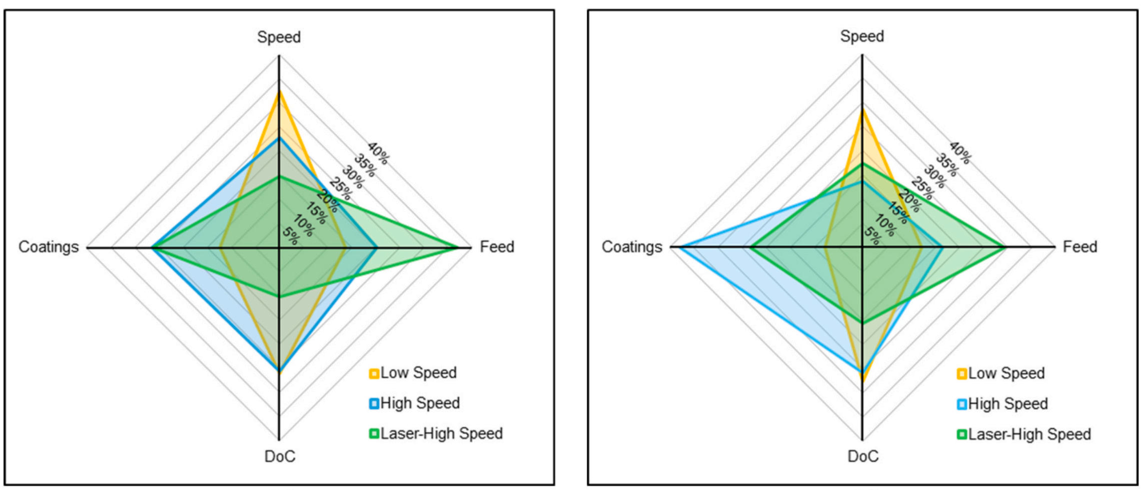


(a) (b)

**Fig. 9.** Comparative analysis of contribution for process parameters across three machining domains against; (a) Burr Width; (b) Burr Height.

**Table 7**
Significance and contribution of process parameters for burr height.

| Source | DF | Seq SS | Contribution | Adj SS | Adj MS | F-Value | P-Value |
|---|---|---|---|---|---|---|---|
| ANOVA at Low Speed | | | | | | | |
| **Speed** | 3 | 21607.5 | 28.54% | 21607.5 | 7202.50 | 7.58 | 0.002 |
| **Feed** | 3 | 9247.7 | 12.21% | 9247.7 | 3082.55 | 3.25 | 0.045 |
| **DoC** | 3 | 20901.0 | 27.61% | 20901.0 | 6967.00 | 7.34 | 0.002 |
| **Coatings** | 3 | 5913.3 | 7.81% | 5913.3 | 1971.12 | 2.08 | 0.137 |
| **Error** | 19 | 18043.0 | 23.83% | 18043.0 | 949.63 | | |
| **Total** | 31 | 75712.5 | 100.00% | | | | |
| ANOVA at High Speed | | | | | | | |
| **Speed** | 3 | 5035.7 | 13.76% | 5035.7 | 1678.56 | 15.18 | 0.000 |
| **Feed** | 3 | 6082.1 | 16.62% | 6082.1 | 2027.35 | 18.34 | 0.000 |
| **DoC** | 3 | 9489.6 | 25.92% | 9489.6 | 3163.19 | 28.61 | 0.000 |
| **Coatings** | 3 | 13896.6 | 37.96% | 13896.6 | 4632.21 | 41.90 | 0.000 |
| **Error** | 19 | 2100.7 | 5.74% | 2100.7 | 110.56 | | |
| **Total** | 31 | 36604.6 | 100.00% | | | | |
| ANOVA at Laser Hybrid High Speed | | | | | | | |
| **Speed** | 3 | 5032.1 | 17.30% | 5032.05 | 1677.35 | 7.60 | 0.002 |
| **Feed** | 3 | 8558.4 | 29.43% | 8558.37 | 2852.79 | 12.93 | 0.000 |
| **DoC** | 3 | 4537.9 | 15.60% | 4537.91 | 1512.64 | 6.86 | 0.003 |
| **Coatings** | 3 | 6764.8 | 23.26% | 6764.75 | 2254.92 | 10.22 | 0.000 |
| **Error** | 19 | 4191.5 | 14.41% | 4191.55 | 220.61 | | |
| **Total** | 31 | 29084.6 | 100.00% | | | | |

further illustrates the role played by coatings in stabilizing shearing action and inhibiting burr development at high speeds. In the laser hybrid high speed domain, feed was labelled as the most dominant factor at 29.43%, followed by coatings (23.26%), speed (17.30%) and depth of cut (15.60%). This standing is in correlation with burr width in the same domain where feed comes at first factor, meaning that laser induced softening changes the dominant mechanism of burr formation to chip load dependence and tool-workpiece interaction.

The trends for burr width and height ranking shown in Fig. 10 are concluded to be same in both low-speed and laser hybrid high-speed domains, where cutting speed is dominant at low speed whereas feed takes control under the laser hybrid conditions. This strong alignment across the two-burr metrics indicates that the mechanisms controlling burr initiation and propagation influence both dimensional attributes in a similar manner. In the high-speed domain, slight differences are visible in Fig. 10(b); for speed and feed they take turns in predominantly contributing to width and height. These dissimilarities are, nevertheless, minor and that the basic order of importance of these influences is not changed. The robustness of the ranking observed for burr width and height in most domains indicates that material flow, chip load, thermal softening and tool-workpiece interaction influence burr width and height simultaneously rather than acting independently. Domain-specific differences arise essentially from different cutting speeds and the addition of laser assistance which changes the equilibrium between mechanical cutting forces and local thermal effects.

### 3.3. Burr trend analysis

#### 3.3.1. Burr width analysis

The effect of process parameters on burr width is presented in the main-effect plots shown in Fig. 11 for low-, high-, and laser hybrid high speed micromilling of Inconel 718. The three domains are easily differentiated. The lowest spindle speed consistently resulted in the highest burr widths, reflecting the inability of lower spindle speeds to cut chips effectively leading to plastically deformed larger burrs. In contrast, the laser-hybrid process has the lowest values indicating that the local softening caused by thermal effects are beneficial for material removal and that burr formation is reduced. High-speed machining offers moderate reduction, benefitting from higher cutting velocities but lacking the thermal softening present in the hybrid mode.

For cutting speed trends shown in Fig. 11(a), all three domains show an inverted-U response: burr width rises to a peak at 7.5 m/min for low speed and drops to minimum value at 10.5 m/min; 100 m/min for high and hybrid and then drops to minimum value at 125 m/min. The decline is most pronounced in the hybrid case, indicating effective thermal–mechanical assistance at higher speeds. The sharp response of burr width to cutting speed in the low-speed domain corresponds well with ANOVA findings, where speed was the most influential parameter. For feed per tooth, trends are domain dependent as shown in Fig. 11(b). In the domain of low-speed, burr width decreases with feed, minimum at 1.5 μm/tooth and then rises, reflecting greater plastic deformation when chip segmentation is poor. High speed domain is non-monotonic, a peak near 2.5 μm/tooth suggests a transition between ploughing and stable shearing while in laser hybrid, burr width drops sharply at the highest feed (3.5 μm/tooth), implying that larger chip load plus laser softening promotes cleaner chip cutting. The significant range observed here is consistent with ANOVA, highlighting feed as the primary influence in the hybrid domain.

Fig. 11(c) illustrates that depth of cut strongly influences burr formation in the low-speed domain, with burr width increasing progressively as undeformed chip thickness rises. In high-speed and hybrid domains, U-shaped trend with a minimum value at 90 μm is observed, however, exhibit relatively stable responses with only modest increases, indicating that elevated cutting speeds and hybrid assistance mitigate the adverse effects of higher material engagement or stabilize chip formation. Fig. 11(d) shows that in the high-speed domain, uncoated tools produced the smallest burrs, while TiAlN gave the largest. This results from sharper edges on uncoated tools reducing ploughing and minimum chip-thickness effects, whereas TiAlN coatings increase edge rounding and burr growth despite its well-known wear resistance. In the hybrid domain, TiAlN coatings achieved the smallest burr widths, while TiSiN performed the worst. This suggests that superior thermal stability and wear resistance of TiAlN coatings allowed it to exploit the softened cutting zone created by laser assistance. Coating effects were less significant at low speed where plastic flow dominates.

The contour interpretation gives a natural display of the joint impact of two factors on serrated burr width and helps to intuitively recognize interaction effects and favorable domain areas. These prescribe minimum and maximum burr regions, indicating zones of robust normal operation. For example, in Fig. 12(a) for low-speed domain, lower feed and higher speed combinations yield small burr width, increased depth of cut tends to increase the size of burrs particularly at high-speed domain as shown in Fig. 12(b). Based on all these findings in a comparative cross-domain analysis it is concluded that burr formation, in principle controlled by cutting mechanics, material's plasticity and thermal effects, finds its balance point changed fundamentally when hybrid laser assistance is applied. It uses a laser to assist in burr width reduction by material softening, providing a substantial advantage over traditional low- and high-speed micro-milling. Taken together, these effects lead to the conclusion that the hybrid technique is more efficient and robust in controlling burr formation in precision micromachining of superalloys.

#### 3.3.2. Burr height analysis

In all three domains, burr height exhibits strong similarities to those observed for burr width, but in some cases, magnitude of variation is less

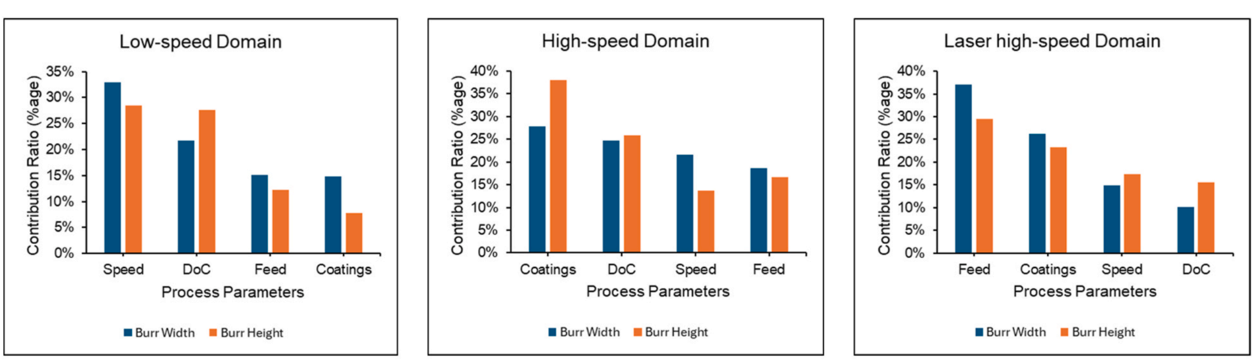


(a) (b) (c)

**Fig. 10.** Comparative analysis of significance for burr width and height across three machining domains; (a) Low-speed domain; (b) High-speed domain; (c) Laser high-speed domain.

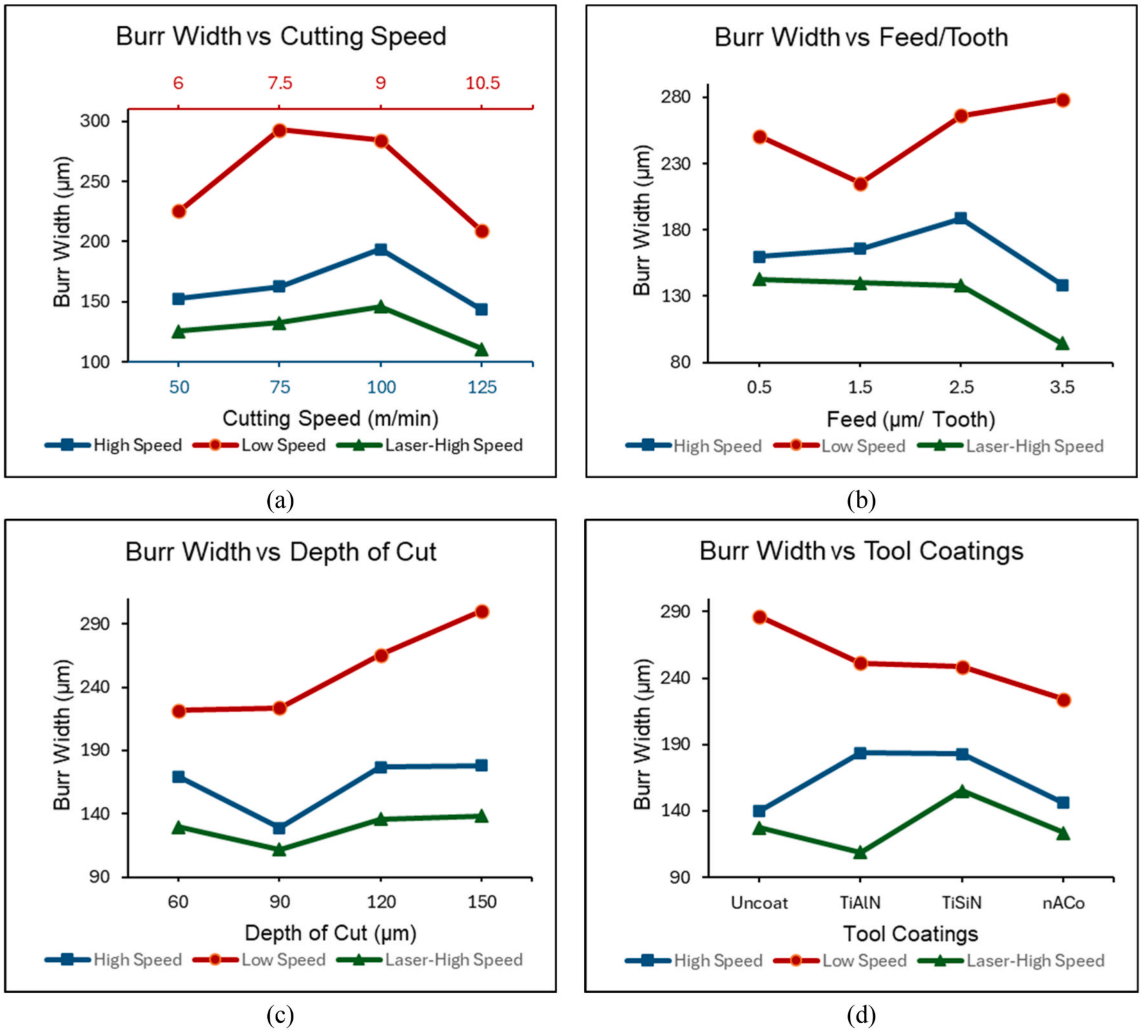


**Fig. 11.** Main effect analysis for burr width: (a) Cutting Speed; (b) Feed; (c) Depth of Cut (d) Tool Coatings.

pronounced. Burr height has a declining trend with the increase of speed like burr width, in high-speed domain as shown in Fig. 13(a), while low speed and hybrid domains presents a non-linear variation. When compared with the burr width, the decrease of burr height is more gradual and shows slightly less sensitivity to speed. For hybrid domain in Fig. 13(b), a particular decrease of burr height occurs for large feeds, as previously observed for burr width but much more suppressed. In contrast, in the low-speed domain, the increase of burr height with feed is more significant than that of burr width, indicating higher susceptibility to chip load for height under conventional conditions.

Regarding depth of cut, trends depicted in Fig. 13(c) for burr height largely mirror those for burr width across all domains. However, the effect is more magnified for burr height at low speed, where increased depth of cut strongly aggravates vertical burr growth. Fig. 13(d) demonstrates that the comparison of coatings' ranking is basically proportional with burr width, though the differences are amplified in magnitude. TiAlN again presented the best performance in the hybrid domain as it reduces burr height profile, while TiSiN remains the worst performer. Interestingly, high-speed superiority of uncoated tools is maintained, proving that the geometry effects dominate coating tribology for both burr width and height.

Collectively, Figs. 11 and 13 show that burr width and height exhibit trend in approximately similar manner across process parameters and machining domains with minor corresponding differences in their magnitudes. In low-speed domain, the burr width and height are also mainly controlled by the cutting speed and depth of cut, but the burr height displays a higher magnifying effect at larger chip loads. At high-speed conditions, the focus of coating varies marginally depending upon width and height, but the priority remains the same in confirming an edge-based geometric impact. In the hybrid domain, TiAlN shows superior performance for both matrices compared to other coatings, indicating that resistance to thermal softening under laser hybrid conditions is critical. In general, burr height is somewhat more influenced by feed and depth than the burr width, yet underlining mechanisms are shared. This dimensionally consistent alignment for Inconel 718 indicates that burr formation is process controlled by common physical principles associated with material flow and chip load, linked with thermal softening with some domain specific differences due to the cutting velocity and use of a laser.

Contour plots provided in Fig. 14 illustrate the collective influence of machining variables on burr height, which made it easy to understand the interaction tendency and zones for minimum burr height. In the low speed cutting range, shown in Fig. 14(a), moderate feeds and intermediate speeds typically result in low burr heights, with higher ones being promoted at higher feeds or depths of cut leading to enhanced plastic deformation. These sensitivities are more prominent for the high-speed domain in Fig. 14(b), where an increased speed results in higher thermal and mechanical loading which leads to larger burrs. With laser assistance in Fig. 14(c), the overall burr-height distribution shifts toward markedly lower levels across the parameter space. Localized thermal softening reduces cutting forces and suppresses the extent of plastic flow which limits the burr growth. Comparatively, the three domains

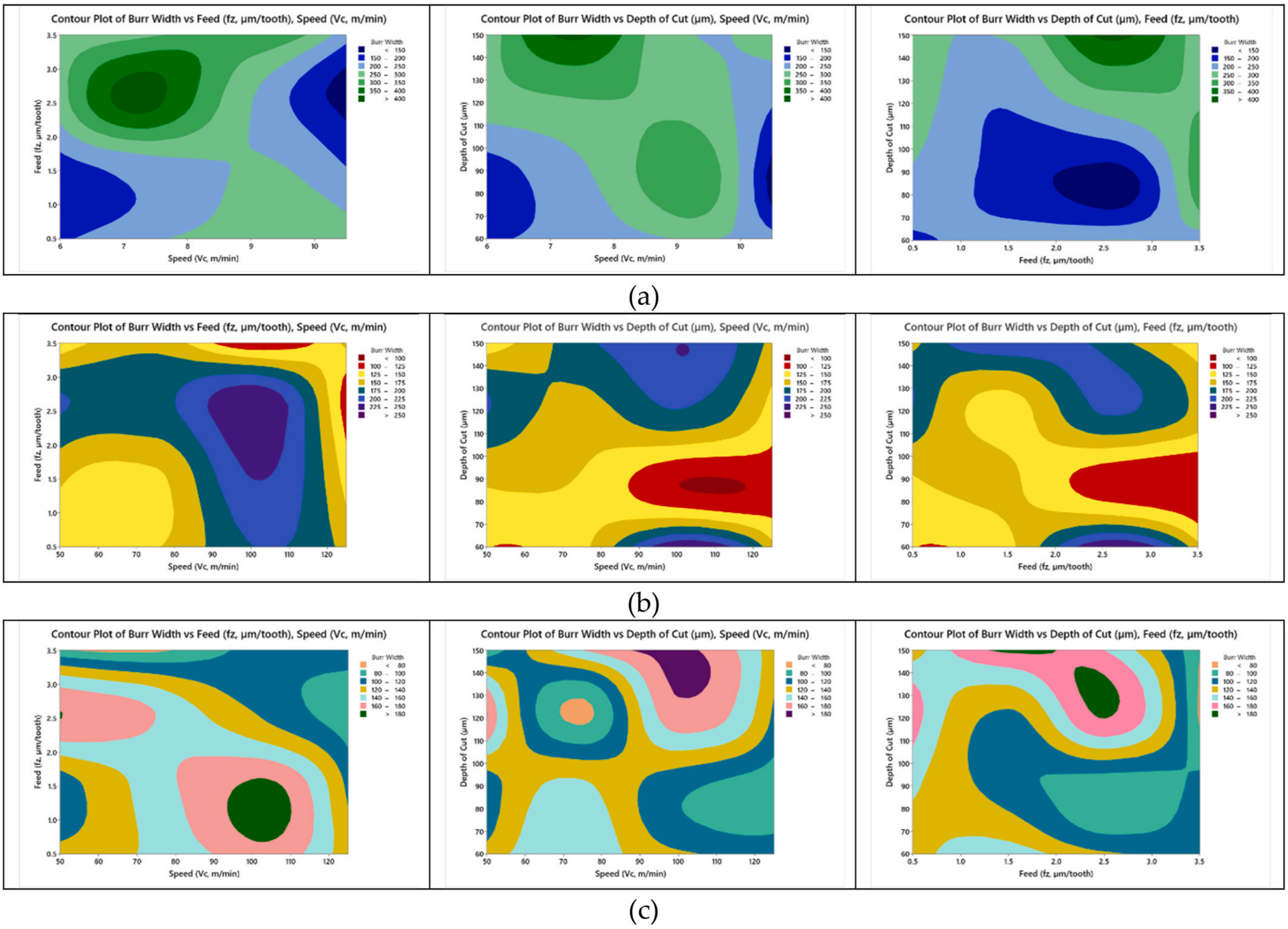


**Fig. 12.** Contour plots of Burr width against machining parameters across three domains: (a) Low speed; (b) High speed; (c) Laser high speed.

demonstrate that although burr height is governed by the interplay of cutting mechanics, thermal effects, and material plasticity, hybrid laser assistance significantly moderates these mechanisms. This establishes the hybrid approach as a more robust and effective strategy for controlling burr height in precision machining of superalloys.

### 3.4. *Validation of ANOVA results*

In this study, optimization for single objective emphasize in minimizing a specific response variable independently for each machining domain under 'smaller-is-better' criterion, without considering interactions or competing objectives. For every domain, the influence of cutting speed, feed rate, depth of cut, and tool coating was examined, and the specific level of each parameter yielding the minimum and maximum burr values was identified from the main-effect trends shown in Figs. 11 and 13. Analysis of main effect plots showed that the most prominent responses depending on parameter settings, indicating their sensitivity in response to different input conditions.

Confirmatory tests were performed for the predicted best and worst parameter combination of each domain for verification to confirm the robustness of the Taguchi experimental design, reported in Table 8 and Table 9 against burr width and height, respectively. The excellent agreement between these predicted Taguchi results with those summarized in Tables 4 and 5 for burr width and height, respectively, confirms strong model fidelity, verifies the validity of the design strategy and substantiates the credibility of the experimental procedure.

## 4. Conclusions

This study presents a comprehensive experimental comparison of burr formation in Inconel 718 across low-speed, high-speed, and novel laser-hybrid high-speed micromachining domains, addressing a gap that has remained insufficiently explored in existing literature. The results demonstrate that burr formation is strongly dependent on the machining domain, with high-speed micromilling offering substantial advantages over low-speed conditions, and laser-hybrid high-speed micromilling delivering the most pronounced burr suppression. The integration of Laser Beam Machining (LBM) as a preconditioning step in the hybrid domain further amplifies these benefits by thermally induced material ablation, reducing cutting resistance, and consistently yielding the smallest burr dimensions across all investigated parameter settings and tool coating strategies. Statistical analysis using ANOVA rigorously establishes the domain-dependent significance of machining parameters in governing burr width and height, highlighting the necessity of domain-specific parameter selection. Overall, the outcomes establish laser hybrid high speed micromilling as an effective and robust strategy for bur control, offering clear advantages in edge quality and reduced post processing requirements. The study underscores the potential of optimized hybrid micro machining as a practical solution for precision manufacturing of nickel-based superalloys with reduced post processing. Key findings are summarized as follows:

1. Cutting speed, tool coating, and feed rate emerged as dominant factors governing burr generation, with their relative contributions

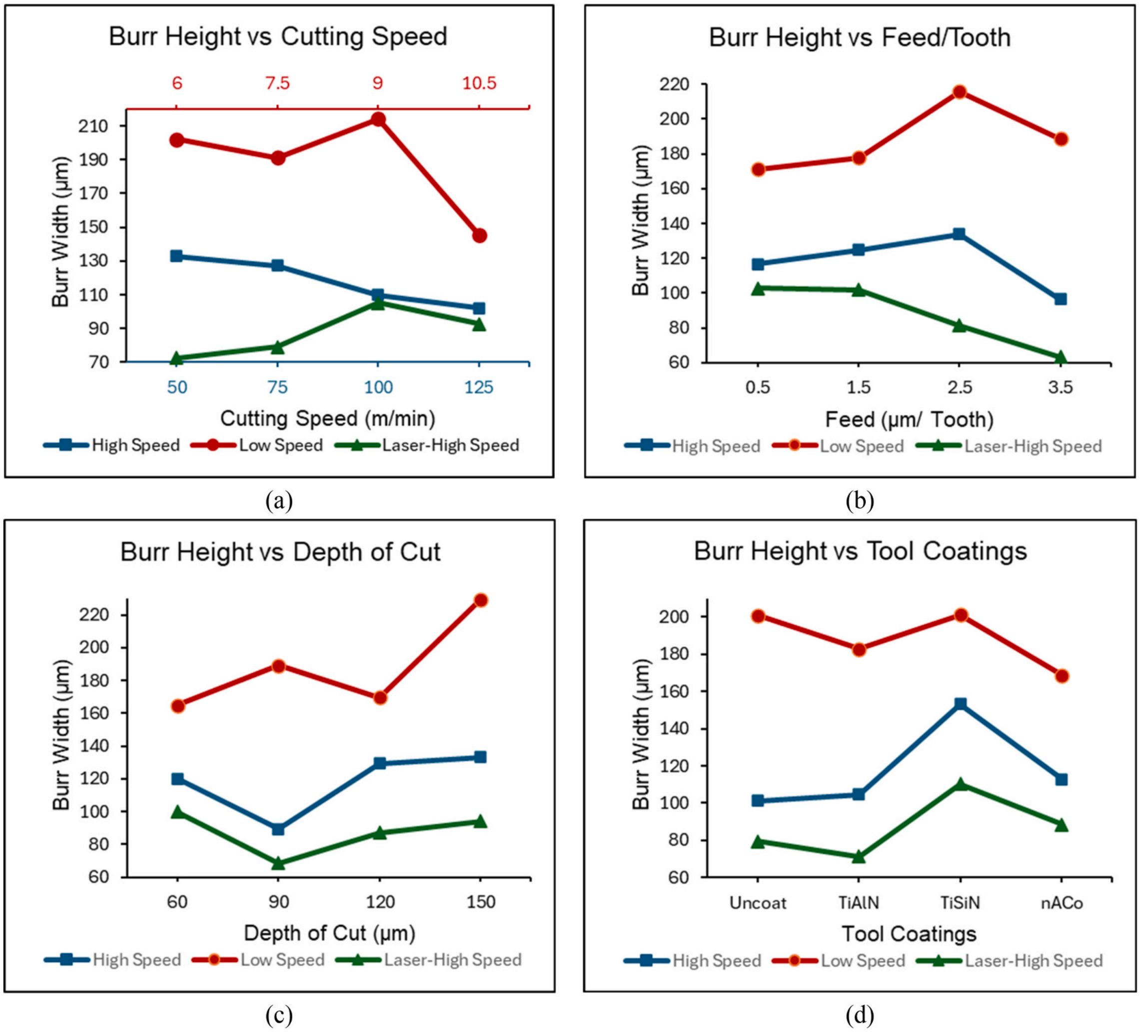


**Fig. 13.** Main effect analysis for burr height: (a) Cutting Speed; (b) Feed; (c) Depth of Cut (d) Tool Coatings.

varying across machining domains. For burr width their contributions were 32.88% in low speed, 27.87% in high-speed domain and 37.05% under laser hybrid conditions, while the corresponding contributions to burr height were 28.54%, 37.96% and 29.43% respectively, highlighting consistently dominant yet domain specific role of these parameters in controlling burr geometry.

2. Tool coating performance was highly domain dependent: nACo coatings provided superior burr suppression under low-speed conditions, uncoated tools performed best in high-speed micromilling and TiAlN coatings demonstrated superior burr suppression in the laser hybrid domain, emphasizing the domain specific tool advantage and underscoring its importance in judicious tool selection.
3. A clear demarcation among machining domains were observed, with the laser hybrid high-speed domain consistently producing the smallest dimensions, the low-speed domain generating the largest burrs, and conventional high-speed micromilling exhibiting intermediate performance.
4. Consistent trends in both burr width and burr height reveal shared suppression mechanisms in the hybrid domain, where localized laser-induced preconditioning reduces cutting resistance and plastic material flow at the edge, enabling burr suppression beyond what can be achieved through high cutting speeds alone.
5. The results demonstrate that machining domain selection governs burr formation to a degree comparable with primary cutting parameters, indicating that process strategy plays a decisive role in edge quality. This elevates the laser hybrid micromachining as an inherently more effective and robust burr suppression approach.

## 5. Future work

Based on the present experimental study, the following future research directions are proposed to further advance hybrid micromachining.

- Meta-heuristic optimization is acknowledged to complement the present experimental framework in future studies to perform global multi-objective optimization of burr width and height using surrogate models derived from the present experimental data. This direction is expected to broaden the applicability and optimization capability of machining strategies for difficult-to-machine materials.
- Extending the present comparative framework to other critical micromachining responses, including surface roughness and tool wear, across low-speed, high-speed, and laser-hybrid domains. Such systematic comparisons are expected to provide a more comprehensive understanding of process-response interactions and to support optimized process selection for miniaturized, high-precision components.

## Consent to participate

There was no human participant involved during the conduct of this

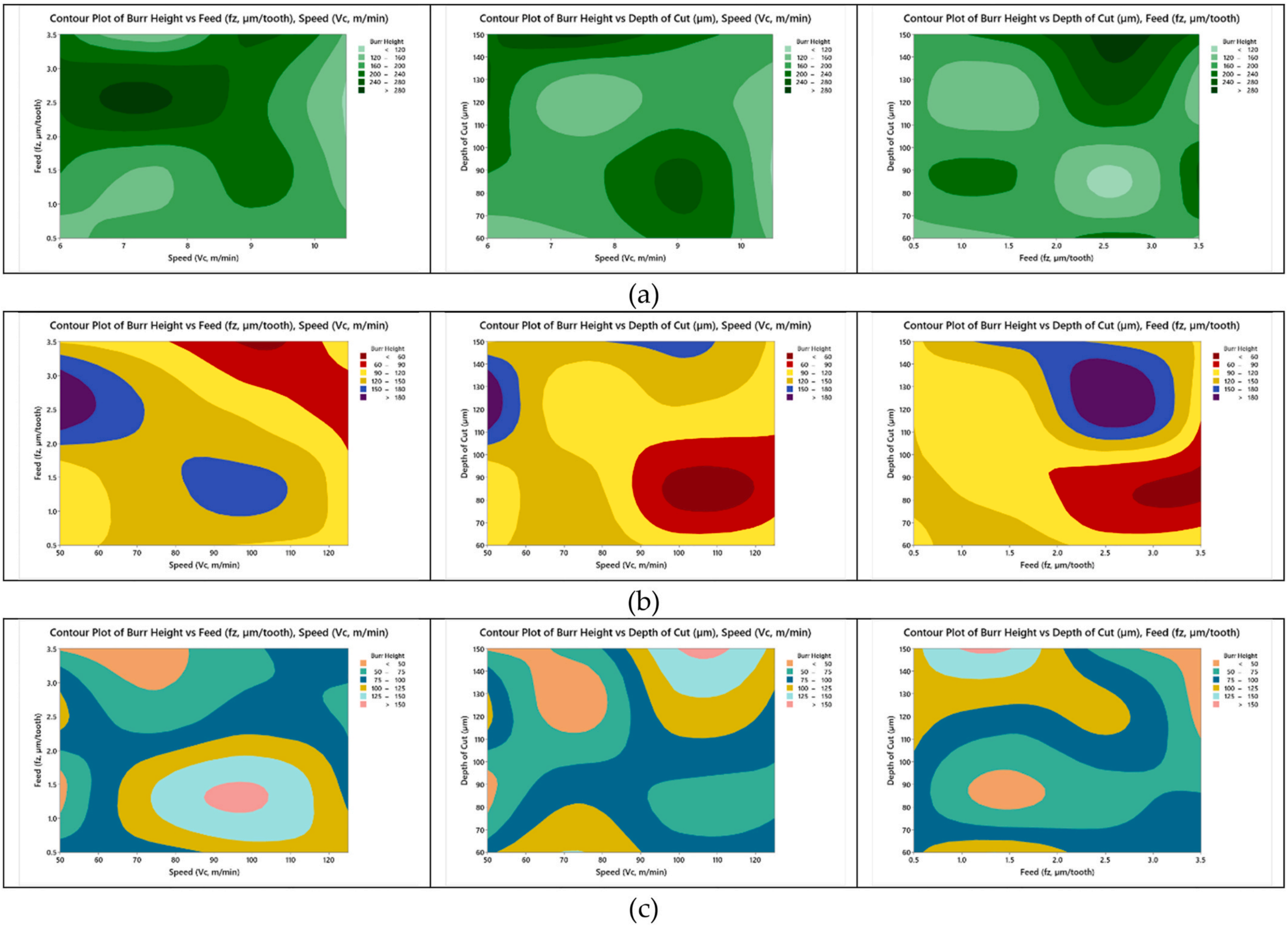


**Fig. 14.** Contour plots of Burr Height against machining parameters across three domains: (a) Low speed; (b) High speed; (c) Laser high speed.

**Table 8**
Optimal input parameter configuration for burr width control.

| Conditions | | Input Parameters | | | | Response |
|---|---|---|---|---|---|---|
| | | Speed *Vc* | Feed *fz* | DoC *ap* | Tool Coatings | Burr Width |
| | | (m/min) | (μm/tooth) | (μm) | (t_c) | (μm) |
| **Low Speed** | **Best** | 10.5 | 1.5 | 60 | nACo | 126.14 |
| | **Worst** | 7.5 | 3.5 | 150 | Uncoat | 421.67 |
| **High Speed** | **Best** | 125 | 3.5 | 90 | Uncoat | 103.71 |
| | **Worst** | 100 | 2.5 | 150 | TiAlN | 251.23 |
| **Laser-High Speed** | **Best** | 125 | 3.5 | 90 | TiAlN | 85.87 |
| | **Worst** | 100 | 0.5 | 150 | TiSiN | 188.17 |

**Table 9**
Optimal input parameter configuration for burr height control.

| Conditions | | Input Parameters | | | | Response |
|---|---|---|---|---|---|---|
| | | Speed *Vc* | Feed *fz* | DoC *ap* | Tool Coatings | Burr Height |
| | | (m/min) | (μm/tooth) | (μm) | (t_c) | (μm) |
| **Low Speed** | **Best** | 10.5 | 0.5 | 60 | nACo | 108.37 |
| | **Worst** | 9 | 2.5 | 150 | TiSiN | 226.18 |
| **High Speed** | **Best** | 125 | 3.5 | 90 | Uncoat | 72.06 |
| | **Worst** | 50 | 2.5 | 150 | TiSiN | 207.96 |
| **Laser-High Speed** | **Best** | 50 | 3.5 | 90 | TiAlN | 40.61 |
| | **Worst** | 100 | 0.5 | 60 | TiSiN | 154.83 |

research.

## Ethics approval

We confirm that this work is original and has not been published elsewhere nor is it currently under consideration for publication elsewhere.

## Consent for publication

All authors consented to submit the outcome of this research for publication in the journal.

## Authors' contributions

Ahmad Waqar Tehami: Conceptualization, Data curation, Formal analysis, Investigation, Methodology, Validation, Writing - original draft. Muhammad Rizwan ul Haq: Conceptualization, DOE, Formal analysis, Visualization, Resources, Supervision, Validation, Writing - original draft. Muhammad Ali Khan: Conceptualization, DOE, Visualization, Formal analysis, Resources, Supervision, Validation, Writing - original draft. Syed Husain Imran Jaffery: Project administration, Resources, Supervision, Validation, Formal analysis, Visualization, Writing - original draft. Muhammad Iftikhar Faraz: Data curation, Formal analysis, Investigation, Project administration, Resources, Writing - original draft. Jana Petru: Conceptualization, DOE, Visualization, Formal analysis, Resources, Writing - original draft.

## Funding

The authors extend their acknowledgement to the financial support of the European Union under the REFRESH-Research Excellence For REgion Sustainability and High-tech Industries project number CZ.10.03.01/00/22_003/0000048 via the Operational Programme Just Transition. This work was supported by the Deanship of Scientific Research, Vice Presidency for Graduate Studies and Scientific Research, King Faisal University, Saudi Arabia (Grant No. KFU260720).

## Declaration of competing interest

The authors declare that they have no known competing financial interests or personal relationships that could have appeared to influence the work reported in this paper.

## Availability of data and material

Data of research is being used for further extended research and can be made available on request.

## References

[1] Schneider F, Das J, Kirsch B, Linke B, Aurich JC. Sustainability in ultra precision and micro machining: a review. Int J Precis Eng Manuf - Green Technol 2019;6: 601–10. https://doi.org/10.1007/s40684-019-00035-2.
[2] Venkatesh V, Swain N, Srinivas G, Kumar P, Barshilia HC. Review on the machining characteristics and research prospects of conventional microscale machining operations. Mater Manuf Process 2017;32:235–62. https://doi.org/10.1080/10426914.2016.1151045.
[3] Unune DR, Mali HS. Current status and applications of hybrid micro-machining processes: a review. Proc Inst Mech Eng Part B J Eng Manuf 2015;229:1681–93. https://doi.org/10.1177/0954405414546141.
[4] Rathod V, Doloi B, Bhattacharyya B. Experimental investigations into machining accuracy and surface roughness of microgrooves fabricated by electrochemical micromachining. Proc Inst Mech Eng Part B J Eng Manuf 2015;229:1781–802. https://doi.org/10.1177/0954405414539486.
[5] dos Santos AG, De Oliveira D, Gomes MC, Jackson MJ, da Silva MB. Correlation between tool wear and machining temperature in micromilling of Ti-6Al-4V alloy. Wear 2025. https://doi.org/10.1016/j.wear.2025.205793.
[6] Lu X, Jia Z, Wang H, Hu X, Li G, Si L. Measurement-based modelling of cutting forces in micro-milling of inconel, 13; 2017. 718.
[7] Xia W, Zhao X, Yue L, Zhang Z. Microstructural evolution and creep mechanisms in Ni-based single crystal superalloys: a review. J Alloys Compd 2020;819:152954. https://doi.org/10.1016/j.jallcom.2019.152954.
[8] Okazaki M, Okazaki M. High-temperature strength of Ni-base superalloy coatings. Sci Technol Adv Mater 2001;6996. https://doi.org/10.1016/S1468-6996(00)00022-X.
[9] Frifita W, Ben Salem S, Haddad A, Yallese MA. Optimization of machining parameters in turning of Inconel 718 nickel-base super alloy. Mech Ind 2020;21. https://doi.org/10.1051/meca/2020001.
[10] Marques A, Guimarães B, Bartolomeu F, Miranda G, Silva FS, Carvalho O. Multi-material Inconel 718 – aluminium parts targeting aerospace applications: a suitable combination of low-weight and thermal properties. Opt Laser Technol 2023;158. https://doi.org/10.1016/j.optlastec.2022.108913.
[11] Ngah N, Kasim MS, Ghanesan HN, Yusof SNA, Mohamed SB, Rahman ZA, et al. A brief review of ultrasonic assisted milling of Inconel 718. J Tribol 2024;40: 14–38.
[12] Takács M, Verö B, Mészáros I. Micromilling of metallic materials. J Mater Process Technol 2003;138:152–5. https://doi.org/10.1016/S0924-0136(03)00064-5.
[13] Lindvall R, Bello Bermejo JM, Bjerke A, Andersson JM, Vikenadler E, M'Saoubi R, et al. On the wear mechanisms of uncoated and coated carbide tools in milling titanium alloys. Int J Refract Met Hard Mater 2024;124. https://doi.org/10.1016/j.ijrmhm.2024.106806.
[14] Chae J, Park SS, Freiheit T. Investigation of micro-cutting operations. Int J Mach Tool Manufact 2006;46:313–32. https://doi.org/10.1016/j.ijmachtools.2005.05.015.
[15] Ullah S, Liang Z, Du Y, Su Z, Guo C, Yin Z, et al. Ultrasonic vibration-assisted micro-milling: a comprehensive review. J Adv Manuf Sci Technol 2024;0:2025009. https://doi.org/10.51393/j.jamst.2025009. 0.
[16] Thepsonthi T, Özel T. Multi-objective process optimization for micro-end milling of Ti-6Al-4V titanium alloy. Int J Adv Manuf Technol 2012;63:903–14. https://doi.org/10.1007/s00170-012-3980-z.
[17] Lee K, Dornfeld DA. Micro-burr formation and minimization through process control. Precis Eng 2005;29:246–52. https://doi.org/10.1016/j.precisioneng.2004.09.002.
[18] Anand KN, Mathew J. Evaluation of size effect and improvement in surface characteristics using sunflower oil-based MQL for sustainable micro-endmilling of Inconel 718. J Brazilian Soc Mech Sci Eng 2020;42:1–13. https://doi.org/10.1007/s40430-020-2239-0.
[19] Zhu XX, Wang WH, Jiang RS, Zhang ZF, Huang B, Ma XW. Research on ultrasonic-assisted drilling in micro-hole machining of the DD6 superalloy. Adv Manuf 2020; 8:405–17. https://doi.org/10.1007/s40436-020-00301-6.
[20] Rauf A, Khan MA, Jaffery SHI, Butt SI. Effects of machining parameters, ultrasonic vibrations and cooling conditions on cutting forces and tool wear in meso scale ultrasonic vibrations assisted end-milling (UVAEM) of Ti–6Al–4V under dry, flooded, MQL and cryogenic environments – a statistical. J Mater Res Technol 2024;30:8287–303. https://doi.org/10.1016/j.jmrt.2024.05.202.
[21] Saxena KK, Qian J, Reynaerts D. A tool-based hybrid laser-electrochemical micromachining process: experimental investigations and synergistic effects. Int J Mach Tool Manufact 2020;155:103569. https://doi.org/10.1016/j.ijmachtools.2020.103569.
[22] Zhang H, Chen F, Li Z, Hu W, Sun T, Zhang J. Investigation of laser-assisted micro-milling process of inconel. 2023. 718.
[23] Romoli L, Vallini R. Experimental study on the development of a micro-drilling cycle using ultrashort laser pulses. Opt Laser Eng 2016;78:121–31. https://doi.org/10.1016/j.optlaseng.2015.10.010.
[24] Ahmed N, Rafaqat M, Pervaiz S, Umer U, Alkhalefa H, Shar MA, et al. Controlling the material removal and roughness of Inconel 718 in laser machining. Mater Manuf Process 2019;34:1169–81. https://doi.org/10.1080/10426914.2019.1615082.
[25] Davim JP. Nontraditional machining processes. n.d..
[26] Hojati F, Azarhoushang B, Daneshi A, Biermann D. Laser pre-structure-assisted micro-milling of Ti6Al4V titanium alloy. Int J Adv Manuf Technol 2022;120: 1765–76. https://doi.org/10.1007/s00170-022-08774-4.
[27] Lauwers B, Klocke F, Klink A, Tekkaya AE, Neugebauer R, McIntosh D. Hybrid processes in manufacturing. CIRP Ann - Manuf Technol 2014;63:561–83. https://doi.org/10.1016/j.cirp.2014.05.003.
[28] Zhang Y, Zhang D, Wu J, He Z, Deng X. A thermal model for nanosecond pulsed laser ablation of aluminum A thermal model for nanosecond pulsed laser ablation of aluminum. https://doi.org/10.1063/1.4995972; 2017.
[29] Ravi-Kumar S, Lies B, Lyu H, Qin H. Laser ablation of polymers: a review. Procedia Manuf 2019;34:316–27. https://doi.org/10.1016/j.promfg.2019.06.155.
[30] Zhao G, Zhao B, Ding W, Xin L. Nontraditional energy-assisted materials and components in aerospace community. A comparative analysis. 2024.
[31] Ahmed N, Darwish S, Alahmari AM. Laser ablation and laser-hybrid ablation processes: a review. Mater Manuf Process 2016;31:1121–42. https://doi.org/10.1080/10426914.2015.1048359.
[32] Qin Y, Brockett A, Ma Y, Razali A, Zhao J, Harrison C, et al. Micro-manufacturing: research, technology outcomes and development issues. Int J Adv Manuf Technol 2010;47:821–37. https://doi.org/10.1007/s00170-009-2411-2.
[33] Zhu L, Yang Z, Xin B, Wang S, Meng G, Ning J, et al. Microstructure and mechanical properties of parts formed by ultrasonic vibration-assisted laser cladding of Inconel 718. Surf Coating Technol 2021;410. https://doi.org/10.1016/j.surfcoat.2021.126964.
[34] Chavoshi SZ, Goel S, Morantz P. Current trends and future of sequential micro-machining processes on a single machine tool. Mater Des 2017;127:37–53. https://doi.org/10.1016/j.matdes.2017.04.057.
[35] Gupta K, Jain NK, Laubscher RF. Overview of hybrid machining processes. SpringerBriefs Appl Sci Technol 2016:1–7. https://doi.org/10.1007/978-3-319-25922-2_1.
[36] Gupta K, Jain NK, Laubscher RF. Hybrid machining processes perspectives on machining and finishing. 2016.
[37] Hamdan A, Sarhan AAD, Hamdi M. An optimization method of the machining parameters in high-speed machining of stainless steel using coated carbide tool for best surface finish. Int J Adv Manuf Technol 2012;58:81–91. https://doi.org/10.1007/s00170-011-3392-5.
[38] Giasin K. Effect of tool coating and cutting parameters on surface roughness and burr formation during micromilling of inconel. 2021. 718.
[39] Baig A, Jaffery SHI, Khan MA, Alruqi M. Statistical analysis of surface roughness, burr formation and tool wear in high speed micro milling of inconel 600 alloy under cryogenic, wet and dry conditions. Micromachines 2023;14. https://doi.org/10.3390/mi14010013.
[40] Siddique MZ, Faraz MI, Butt SI, Khan R, Petru J, Husain S, et al. Parametric analysis of tool wear , surface roughness and energy consumption during turning of inconel 718 under dry , wet and MQL conditions. 2023.
[41] ul hasan S, Ali S, Jaffery SHI, ud Din E, Mubashir A, Khan M. Study of burr width and height using ANOVA in laser hybrid micro milling of titanium alloy (Ti6Al4V). J Mater Res Technol 2022. https://doi.org/10.1016/j.jmrt.2022.11.051.
[42] Faraz MI, Petru J. Evaluation of machining variables on machinability of nickel alloy inconel 718 using coated carbide tools. 2024.
[43] Sheheryar M, Khan MA, Jaffery SHI, Alruqi M, Khan R, Bashir MN, et al. Multi-objective optimization of process parameters during micro-milling of nickel-based alloy inconel 718 using Taguchi-grey relation integrated approach. Materials (Basel) 2022;15. https://doi.org/10.3390/ma15238296.
[44] Kharche PP, Patil VH. Laser beam machining - an overview. Int J Innov Eng Sci 2021;6:168. https://doi.org/10.46335/ijies.2021.6.10.35.
[45] Sargar TS, Gautam NK, Jadhav AB. Laser beam machining: a review on research trend. Int J Renew Energy Exch 2023;11:1–8. https://doi.org/10.58443/ijrex.11.1.2023.1-8.
[46] Pramanik A, Basak AK. Laser beam machining of titanium alloy—A review. Metals (Basel) 2023;13:1–16. https://doi.org/10.3390/met13091536.

[47] Dubey AK, Yadava V. Laser beam machining-A review. Int J Mach Tool Manufact 2008;48:609–28. https://doi.org/10.1016/j.ijmachtools.2007.10.017.
[48] Cardoso P, Davim JP. A brief review on micromachining of materials. Rev Adv Mater Sci 2012;30:98–102.
[49] O'Toole L, Kang CW, Fang FZ. Precision micro-milling process: state of the art. Adv Manuf 2021;9:173–205. https://doi.org/10.1007/s40436-020-00323-0.
[50] Singh R, Melkote SN. Characterization of a hybrid laser-assisted mechanical micromachining (LAMM) process for a difficult-to-machine material. Int J Mach Tool Manufact 2007;47:1139–50. https://doi.org/10.1016/j.ijmachtools.2006.09.004.
[51] Bilgin M, Karabulut Ş, Karakoç H, Kayır Y, Sarıkaya M. An experimental investigation on machining-induced surface/subsurface characteristics of nickel based Inc-718 alloy: a novel hybrid approach in milling process. Tribol Int 2024;191. https://doi.org/10.1016/j.triboint.2023.109120.
[52] Jain K, Tak M, Mote RG. Impact of surface micro-dimples on machinability of Inconel 718 alloy. https://doi.org/10.1063/10.0028754; 2025.
[53] Ezugwu EO, Wang ZM, Machado AR. The machinability of nickel-based alloys: a review. J Mater Process Technol 1998;86:1–16. https://doi.org/10.1016/S0924-0136(98)00314-8.
[54] Martins H, Puga H. Ultrasonic assisted machining overview: accessing feasibility and overcoming challenges for milling applications. Metals (Basel) 2023;13. https://doi.org/10.3390/met13050908.
[55] Camposeco-negrete C. Optimization of cutting parameters for minimizing energy consumption in turning of AISI 6061 T6 using Taguchi methodology and ANOVA. J Clean Prod 2013. https://doi.org/10.1016/j.jclepro.2013.03.049.
[56] Tehami AW, Haq MR ul, Khan MA, Jaffery SHI, Faraz MI, Petru J. Machinability analysis of Inconel 718 through parametric optimization using novel laser hybrid micro milling technique. Mater Today Commun 2026;50:114387. https://doi.org/10.1016/j.mtcomm.2025.114387.
[57] Aramcharoen A, Mativenga PT. Size effect and tool geometry in micromilling of tool steel. Precis Eng 2009;33:402–7. https://doi.org/10.1016/j.precisioneng.2008.11.002.
[58] Brandão F, Oliveira D, Roger A, Teixeira R, Fagali A, Souza D. Size effect and minimum chip thickness in micromilling. Int J Mach Tool Manufact 2015;89:39–54. https://doi.org/10.1016/j.ijmachtools.2014.11.001.
[59] N AK, Mathew J. Size effect and micro endmilling performance while sustainable machining on Inconel 718. Mater Manuf Process 2021;36:668–76. https://doi.org/10.1080/10426914.2020.1854465.
[60] Jaffery SHI, Khan M, Ali L, Mativenga PT. Statistical analysis of process parameters in micromachining of Ti-6Al-4V alloy. Proc Inst Mech Eng Part B J Eng Manuf 2015;230:1017–34. https://doi.org/10.1177/0954405414564409.
[61] Mehta V, Potdar P, Joshi A. Hybrid AHP-TOPSIS approach for selecting optimal aluminium matrix in casting of metal matrix composites. Opsearch 2025. https://doi.org/10.1007/s12597-025-01079-6.
[62] Jagdale M, Abdullah M, Ambhore N, Kulkarni A, Chaudhari R, Vora J, et al. Performance evaluation and multi-objective optimization of EDM parameters for Ti6Al4V using different tool electrodes. Sci Rep 2025;15:1–18. https://doi.org/10.1038/s41598-025-15756-5.
[63] Dutta S, Sarma DK, Vora J, Chaudhari R, Bhowmik A, Samal P, et al. A state-of-the-art review on micro-machining of nitinol shape memory alloys and optimization of process variables considering the future trends of research. J Manuf Mater Process 2025;9:1–50. https://doi.org/10.3390/jmmp9060183.
[64] Zhang Z, Wu F, Wu A. Research on multi-objective process parameter optimization method in hard turning based on an improved NSGA-II algorithm. Processes 2024;12. https://doi.org/10.3390/pr12050950.
[65] Joshi M, Ghadai RK, Madhu S, Kalita K, Gao XZ. Comparison of nsga-ii, moalo and moda for multi-objective optimization of micro-machining processes. Materials (Basel) 2021;14:1–15. https://doi.org/10.3390/ma14175109.
[66] Chen MJ, Ni HB, Wang ZJ, Jiang Y. Research on the modeling of burr formation process in micro-ball end milling operation on Ti-6Al-4V. Int J Adv Manuf Technol 2012;62:901–12. https://doi.org/10.1007/s00170-011-3865-6.
[67] Sankeerth A, Pagidi K, Gurabvaiah M, Chilakalapalli P, Prakasa S, Barmavatu P, et al. Laser-assisted machining of niobium alloy (C-103): effects of process parameters on cutting force and surface finish. 2025.
[68] Hafiz MSA, Kasim MS, Mohamad WNF, Izamshah R, Aziz MSA, Akmal M, et al. Machinability ultrasonic assisted milling of inconel 718 by using taguchi method. ARPN J Eng Appl Sci 2018;13:8221–6.
[69] Buckner CA, Lafrenie RM, Dénommée JA, Caswell JM, Want DA, Gan GG, et al. Ultrasonic assisted machining of nickel-based superalloy inconel 718. Intech 2018;11:13.
[70] He Y, Zhou Z, Zou P, Gao X, Ehmann KF. Study of ultrasonic vibration–assisted thread turning of Inconel 718 superalloy. Adv Mech Eng 2019;11:1–12. https://doi.org/10.1177/1687814019883772.